2013

Correcting heat flow data in the United States to account for climate change

Godswill Njoku
University of North Dakota

CORRECTING HEAT FLOW DATA IN THE UNITED STATES TO ACCOUNT FOR CLIMATE CHANGE

by

Godswill O. Njoku
Bachelor of Technology,
Federal University of Technology Owerri, Nigeria 2006

A Thesis

Submitted to the Graduate Faculty

of the

University of North Dakota

in partial fulfillment of the requirements

for the degree of

Master of Science

Grand Forks, North Dakota
December
2013

This thesis, submitted by Godswill O. Njoku in partial fulfillment of the requirements for the Degree of Master of Science from the University of North Dakota, has been read by the Faculty Advisory Committee under whom the work has been done and is hereby approved.

_____
Dr. William Gosnold, Chairperson

_____
Dr. Richard LeFever

_____
Dr. Nels Forsman

This thesis is being submitted by the appointed advisory committee as having met all the requirements of the School of Graduate Studies at the University of North Dakota and is hereby approved.

_____
Wayne Swisher
Dean of the School of Graduate Studies

_____
Date

PERMISSION

Title	Correcting Heat Flow Data in the United States to Account for Climate Change
Department	Geology and Geological Engineering
Degree	Master of Science

In presenting this thesis in partial fulfillment of the requirements for a graduate degree from the University of North Dakota, I agree that the library of this University shall make it freely available for inspection. I further agree that permission for extensive copying for scholarly purposes may be granted by the professor who supervised my thesis work or, in his absence, by the Chairperson of the department or the dean of the School of Graduate Studies. It is understood that any copying or publication or other use of this thesis or part thereof for financial gain shall not be allowed without my written permission. It is also understood that due recognition shall be given to me and to the University of North Dakota in any scholarly use which may be made of any material in my thesis.

Godswill O. Njoku
November 1, 2013

TABLE OF CONTENTS

LIST OF FIGURES

LIST OF TABLES

ACKNOWLEDGEMENTS

My deep appreciation goes to Dr. Gosnold for his huge intellectual support towards my research and also to my committee members, Dr. LeFever and Dr. Forsman. Thank you to the geothermal team, most especially Aaron Ochsner and Mark MacDonald for their support. I would like to thank Prosper Gbolo for his encouragement. Thanks to my parents and siblings for believing in me. Finally, I would like to thank my lovely wife, Chidinma Njoku for her care, support and encouragement through these times.

ABSTRACT

Heat flow measurements may require correction for both recent warming and post-glacial warming signals. Warming during the last century can be detected in borehole temperature profiles. Both climate warming signals during the past century and post-glacial warming signals during the past 10 millennia are greatest near the surface and diminish with depth.

Both atmospheric data and borehole temperature data show that recent warming varies systematically with latitude along a north-south transect in the United States. The systematic increase with latitude from +0.7 ^{o}C at 41.6^{o}N to +2.3 ^{o}C at 49^{o}N during the last century is consistent with the prediction that global warming due to increasing amount of CO_2 in the atmosphere varies with latitude.

A systematic increase of heat flow with depth is predicted to result from the post-glacial warming signal in the upper 2km. A modeled depth dependent correction of post-glacial warming indicated that the thermal gradient may be underestimated by 27% in some areas, thereby implying that some heat flow values in the United States may be up to 27% higher depending on the depth of the temperature gradient measurement. Averaging the corrected heat flow values shows that the average heat flow is 58 mW m^{-2}, 78 mW m^{-2} and 51 mW m^{-2} for the whole conterminous United States, Western and Eastern United States respectively.

CHAPTER I

INTRODUCTION

Hypothesis

The importance of analyzing the United States heat flow database to test that the heat flow previously studied, showing a systematic increase of heat flow with depth, may be a result of post-glacial warming, cannot be over emphasized. I hypothesize that the systematic increase of heat flow with depth is a result of climate change, particularly the effect of post-glacial warming.

Correction of heat flow data to accurately account for the effect of climate change will have a significant impact on the heat flow data base and interpretations of heat flow relevant to, enhanced geothermal energy systems, maturation of hydrocarbons, and other related geophysical research, all of which are a function of the distribution of temperature in the upper few hundred kilometers of Earth.

Overview

Over the last century there has been an increase in ground surface temperature due to climate warming and the signal is observed in borehole temperature profiles. In practice, terrestrial heat flow is determined using temperature profiles measured in segments of a borehole exhibiting a linear gradient and from which core samples have been acquired to measure thermal conductivity. Approximately 90% of these T-z

measurements were made in the upper few hundred meters of the crust where major effect of climate change would cause temperature gradients to be disturbed.

The post-glacial warming signal is greatest near the surface and diminishes with depth, hence heat flow determinations in shallow boreholes tend not to provide accurate heat flow data. “The ground surface temperature (GST) varies regularly on diurnal, seasonal, and annual scales and irregularly in response to synoptic weather patterns, interannual climate variability and long-term climate change.” (Gosnold et al., 1997).

Heat Flow

Heat flow is conduction of heat from a warmer to a cooler area according to Fourier’s law $q = \lambda\Gamma$, where q is the heat flow (mW m^{-2}), λ is thermal conductivity (W m^{-1} K^{-1}), and Γ is geothermal gradient (mK m^{-1}). The sources of heat in the crust and mantle are radioactive heat production from U, Th and K and residual heat acquired during accretion of the planet from the solar nebula. The temperature gradient and thermal conductivity are two important measurements required for the computation of heat flow. The temperature gradient measurements can be obtained from borehole temperature depth profile, while thermal conductivity is measured from rock samples.

Previous Studies

In 1939, Bullard and Benfield individually reported the first continental heat flow measurements. Cermak (1971) carried out a comprehensive borehole climate reconstruction by inversing temperature measurements in deep boreholes in Canada to reconstruct their climate history. In the twentieth century, researchers’ interest in climate change and how it affects the thermal gradient estimates grew (Cermak et al., 1992). Thus, temperature history resulting from climate change was reconstructed to determine

the disturbed subsurface temperature and temperature gradients (Lachenbruch & Marshall, 1986; Deming, 1995; Majorowicz & Safanda, 1998).

Previous work (e.g., Blackwell (1971, 1978); Lachenbruch & Sass (1978, 1980, 1992); Roy et al., 1972; Morgan & Gosnold, 1989; Gosnold, 1990; Blackwell et al., 1991; Reiter et al., 1991) has established a general summary of the heat flow in the United States. The majority of the heat flow data are concentrated in the tectonically young western part of the United States. Studies have shown that heat flow is variable but generally high within the western region particularly in the Basin and Range province which is characterized by high heat flow that extends to within 10 to 20 km of the eastern scarp of the Sierra Nevada (Sass et al., 1971) (Figure 1.)

In contrast, fewer heat flow measurements have been made within the eastern United States (Figure 2) which is a result of researchers' interests in young tectonically active areas rather than stable areas. The distribution of heat flow within the tectonically active western United States and quiet eastern United States is shown in Figure 1. Most heat flow values range between 40-60mW/m^2 for a stable craton in the United States and the average heat flow value for western United States and the United States as a whole is 75mW/m^2 and 55mW/m^2 respectively (Wisian et al., 1999).

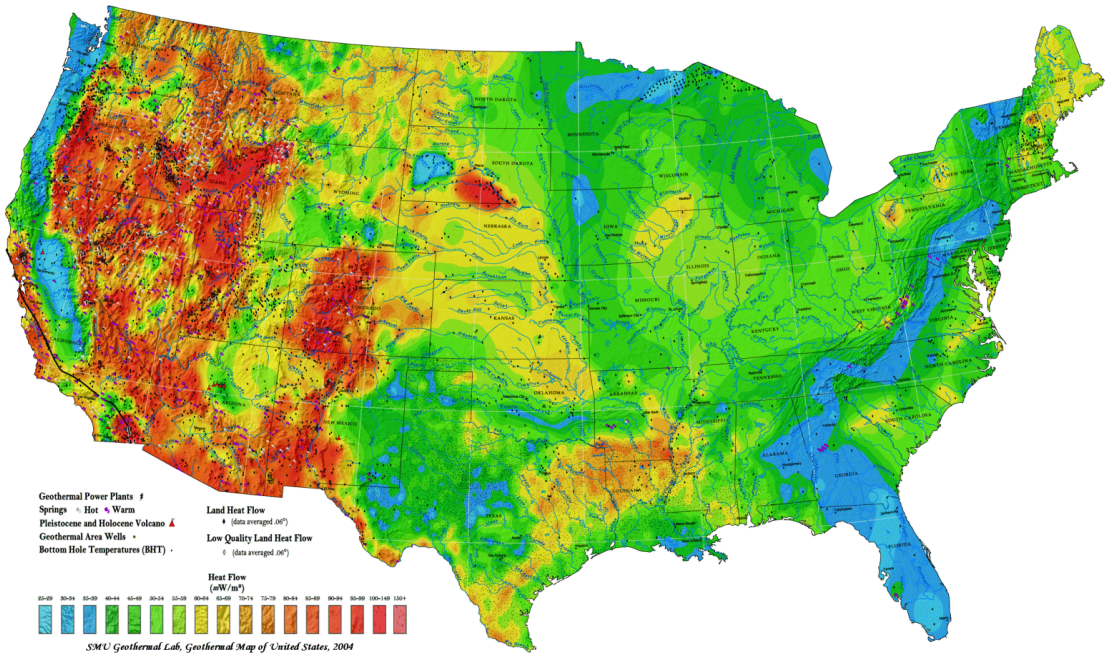

Figure 1. Heat flow map of the United States. (Blackwell and Richards, 2004)

The relationship between heat flow and heat production in an area where the tectonic history is somewhat similar is defined as a heat flow province (Blackwell, 1971). The division of heat flow of the United States based on physiographic province has been presented by various authors (e.g., Roy et al., 1968; Sass et al., 1971; Morgan &Gosnold, 1989). Although the heat flow in the western United States is generally high, the surface heat flow pattern is not controlled everywhere by province boundaries (Morgan & Gosnold, 1989). Different factors ranging from ground water recharge, subduction, elevation, faulting, radioactive decay to tectonic activities all are reasons for the low to high heat flow within the United States provinces. In addition, crustal thickness, distribution of heat producing elements and erosion also affect regional heat flow (Lachenbruch, 1970; Sclater et al., 1980).

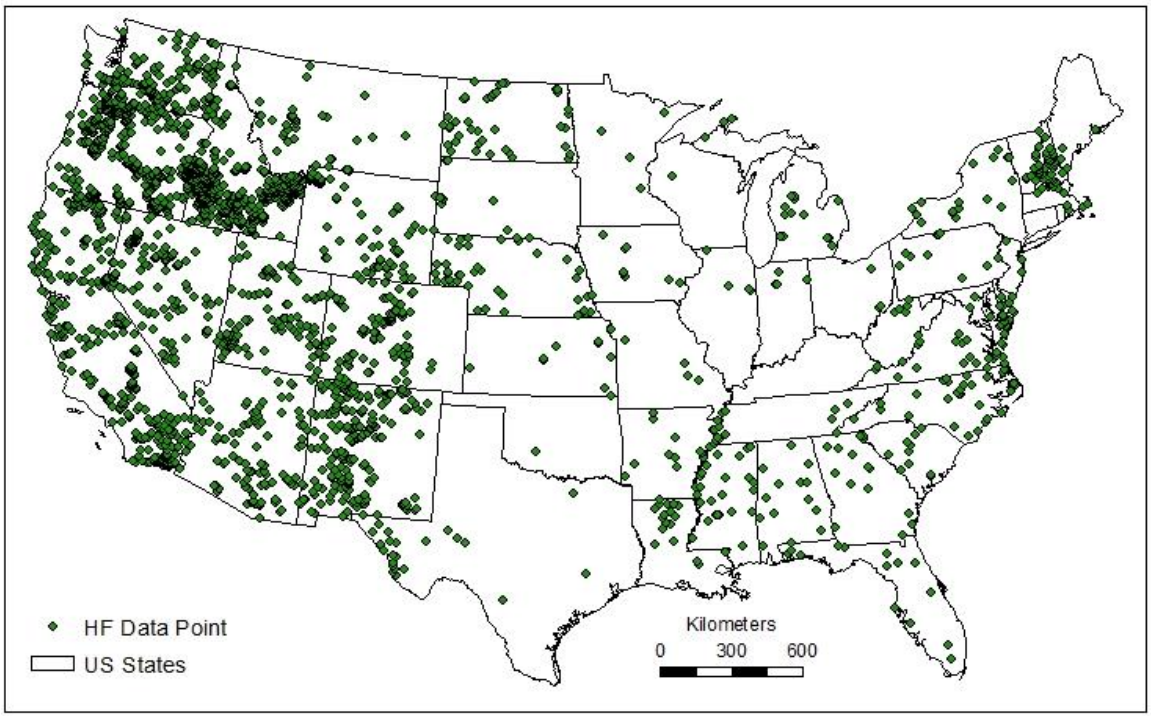

Figure 2. Heat flow data of the conterminous United States as of 2013. (Data source: SMU-UND United States Heat Flow Database)

Climate Change and Borehole Temperature Profiles

Understanding climate change is important because it allows placing climate change in the context of other large challenges facing the world. Climate change on time scales of centuries to millennia can be caused by changes in solar radiation, oceanic circulation, and by changes in atmospheric composition, e.g. volcanic eruptions and anthropogenic greenhouse gases.

Increase in proportion of greenhouse gases as a result of the rise in atmospheric concentration of CO_2 and other infrared absorbing gases contributes to global warming. Since the past 400 millennia, as carbon dioxide rises, the air temperature rises; as carbon dioxide falls, the air temperature falls (Ochoa et al., 2005). The greenhouse gas

concentration generated by human activities accounts for the warming observed in the last 50 years (Ochoa et al., 2005).

The average surface temperature has increased considerably by about 0.6^{o}C (1.1^{o}F) during the twentieth century (Ochoa et al., 2005). The increase in temperature during the twentieth century in the North Hemisphere was greater than any other century in the last thousand years. This temperature change has not been uniform across the globe but has varied from region to region. It has since been proven that noise signals affecting the top few hundred meters of subsurface temperature data are as a result of climate change. Consequently, borehole temperature data shows climate change clearly when conditions like topography, groundwater flow and other anthropogenic conditions are favorable.

Globally, about 680 heat flow borehole temperature data that have been analyzed for evidence of surface temperature changes have shown common patterns of near surface perturbation, indicating that temperature fluctuations at the surface have been propagating downward into the subsurface (e.g., Cermak, 1971; Beck, 1977; Lachenbruch & Marshall, 1986; Beltrami & Mareschal, 1991; Wang, 1992; Wang & Lewis, 1992; Pollack & Chapman, 1993; Harris & Chapman, 1995; Deming, 1995; Clauser & Mareschal, 1995; Shen et al., 1996; Gosnold et al., 1997; Clow, 1998; Majorowicz & Safanda, 1998). Information about Earth's changing surface temperature, particularly the effect of climate change, can be extrapolated from borehole temperature-depth profiles.

Gosnold et al. (1997) showed a warming trend over the last century that increased systematically with latitude in the mid-continent of North America. They concluded that

ground surface warming increased from +0.4^{o}C at 41.1^{o}N to +2.0^{o}C at 49.6^{o}N and the surface air temperature warmed from +0.5^{o}C per century at 40^{o}N to +1.6^{o}C per century at 48.8^{o}N during the last century. Previous investigation has shown that the warming trend of eastern Canada extends to the north of the Cordillera (Majorowicz & Safanda, 1998).

Birch (1948) and Beck (1977) both presented a post-glacial warming correction of heat flow data concluding that heat flow measurements made in the upper few hundred meters would show the effect of warming, therefore causing their temperature gradients to be underestimated. Although, several heat flow researchers reported the effect of climate warming on heat flow data to be totally insignificant due to the slight degree of warming (Sass et al., 1971; Wang, 1992; Huang et al., 1997), recent palaeoclimate corrections of heat flow data across different continents have been determined to have significant impact (e.g., Slagstad et al., 2009; Majorowicz & Wybraniec, 2011; Westaway & Younger, 2013). However, the heat flow data across the United States requires correction for the effects of post-glacial warming before they can give precise quantification of geothermal energy resources.

CHAPTER II

RESEARCH METHODS

Heat Flow Data Set

The heat flow data set utilized in this research resides in the Southern Methodist University and University of North Dakota (SMU-UND) United States Heat Flow Database. As of 2013, the updated United States heat flow data set includes more than 4,000 observations. The non-uniformity of the data set can be seen from the geographical location of the heat flow measurement sites (Figure 2.). About 85% includes the actual depth range (minimum and maximum values) over which the measurement was made.

My analysis offers a thorough and careful assessment of the data set for research purposes. The measurements made at the minimum depth were used as the actual depth of measurement. Since climate signals over the last 25,000 years are largely retained in the upper 2,000m, only measurements from depths between 100 - 2,000m were analyzed. Also, the exclusion of heat flow values in excess of 200mWm^{-2} was done due to the effect of advective disturbances associated with regions of high thermal gradients. A total of 2,897 heat flow observation sites from the database including their thermal conductivity, thermal gradient and heat flow values for each sites passed this screening (Figure 3.).

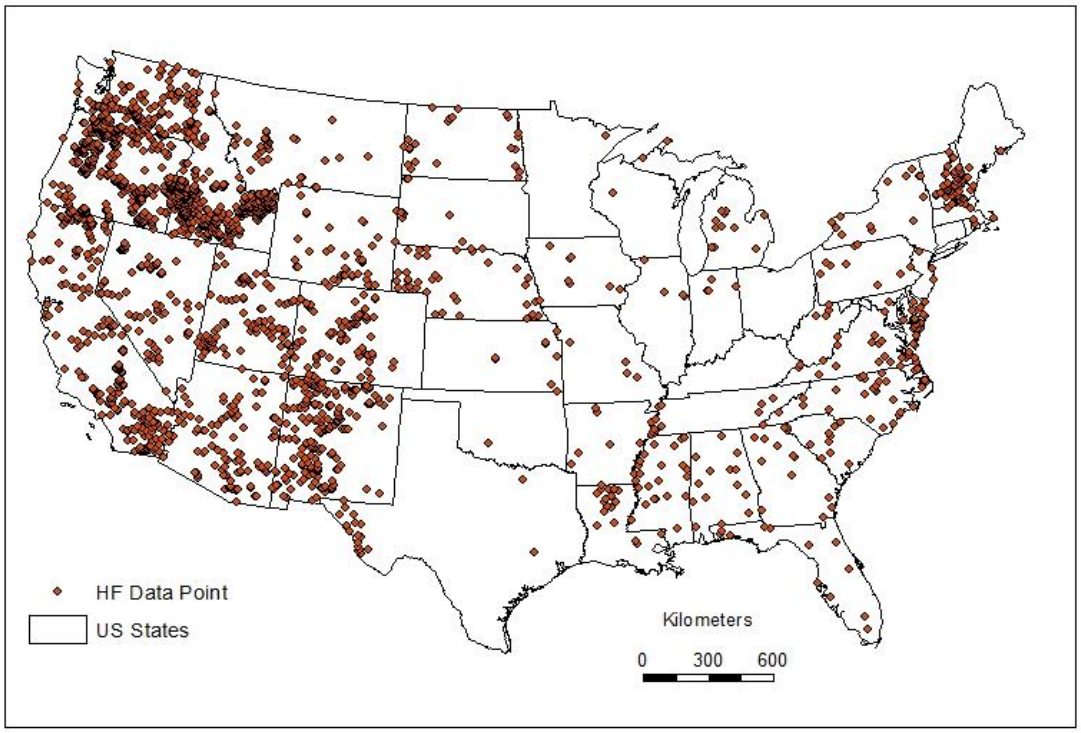

Figure 3. Map showing the heat flow data measurement locations selected for analysis. (Data source: SMU-UND United States Heat Flow Database 2013)

Physiographical Provinces

The United States heat flow data set was characterized province by province to generalize the distribution of heat flow values. There are a total of 24 physiographic provinces within the United States used for this research and slightly more than half are in the eastern part of the United States (Appendix A). An average heat flow value for the western and eastern United States can be calculated from the areally averaged data with each physiographic province. Areal averaging is necessary due to the high concentration of heat flow observation sites in the west. The Great Plains province boundary forms a demarcation between the western and the eastern United States as shown in Figure 4.

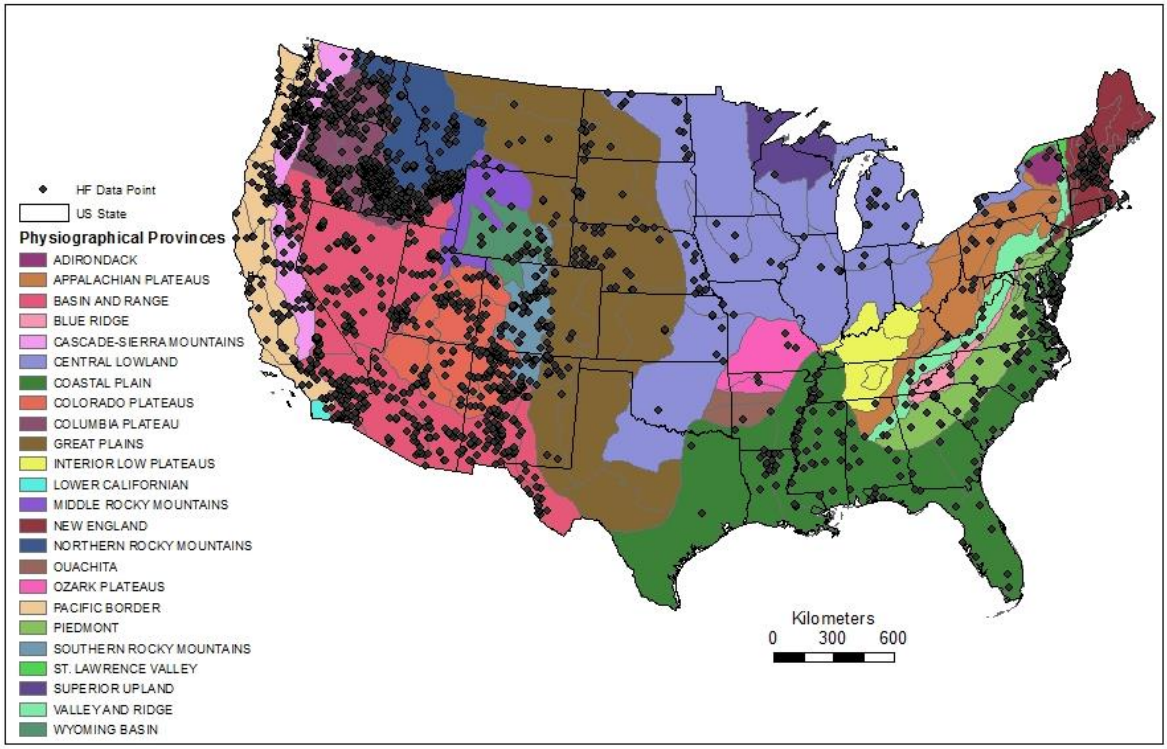

Figure 4. Map showing the heat flow data measurement locations and major physiographical provinces selected for analysis. (Data source: SMU-UND United States Heat Flow Database 2013)

Recent Warming Correction Scheme

Since the climate cools poleward proportional to latitude, the amplitude of climate change induced by recent warming is predicted to increase poleward. Data of the mean annual temperature was gathered from the National Climatic Data Center (NCDC). The plot of the north-south transect of the central (32.5^{o}N - 47.5^{o}N), west-central (38.5^{o}N - 47.5^{o}N) and east-central (35.5^{o}N - 47.5^{o}N) United States mean annual temperature data showed recent warming signals.

From the plotted graph of temperature versus time of each north-south transect, the change in temperature for each north-south transects was computed using linear regression. A mid-point of the latitude representing each state in the north-south transect

was computed to test for a significant correlation with the warming. Interestingly, the graph of warming versus latitude of the north-south transect agreed with the systematic increase in warming with latitude. The equation of the trend line fit into the graphs was used as the latitude dependent correction scheme for the effect of recent warming signals in the last century.

Palaeoclimate Correction Scheme

In North America, only about 15% of all heat flow measurements were made at depths greater than 2, 000m and about 80% of the heat flow data has been greatly underestimated due to post glacial warming signals in shallow depth. Consequently, the effect of post glacial warming is greatest near the surface and diminishes with depth.

Jessop (1971) developed a surface adjustment climate warming correction scheme that was not depth dependent. A model of temperature variations and the diffusive character they propagate into the ground were developed by Carslaw and Jaeger (1959).

$$T_\theta = T_0 \, erfc\left(\frac{z}{\sqrt{4kt}}\right) \qquad \text{(Eq. 2.1)}$$

In the above equation, $\mathbf{T}_\theta$ (^{o}C) is the departure from original equilibrium temperature at depth **z** (m), $\mathbf{T_0}$ is the change in surface temperature (^{o}C), **k** is the thermal diffusivity (m^2/s), **erfc** (x) is the complimentary error function and **t** is time in years. Using the above equation in modeling the surface temperature variation and the impact on the near surface temperature gradient, it predicts an estimated change due to an abrupt change in temperature at a point in time. Heat flow values were then corrected for post-glacial warming by applying the percentage difference due to the magnitude of change in the geothermal gradient.

Geographic Information Science (GIS) techniques were used to generate maps and estimates of the average heat flow based on provinces. GIS allowed a critical evaluation of the heat flow data based on their matching provinces, enabling an average corrected heat flow values in the United States based on individual provinces to be derived. Using ArcGIS 10 with Excel, calculated mean, standard deviation and corrected heat flow values were derived. Graphs were also produced using Excel.

CHAPTER III

RESULTS AND DISCUSSION

Heat Flow Variation With Depth

Increase in heat flow with depth has been observed by previous research (e.g. Kukkonen, Gosnold, & Safanda, 1998; Kukkonen & Joeleht, 2003; Safanda, Szewczyk, & Majorowicz, 2004). About 2,900 heat flow values at different depth in different boreholes across the United States show a systematic increase with depth (Figure 5). Heat flow variations with depth can be interpreted to be a result of the many factors, such as topography, vertical and horizontal water flows, thermal conductivity anisotropy, convective heat transfer and ground surface temperature changes.

In this study, I predict that the systematic variation in heat flow value with depth is mainly due to a paleoclimatic effect caused by ground surface temperature changes during the Last Glacial Maximum (LGM). Heat flow values need to be corrected for the effect of the above mention factors to obtain a significant database useful in comprehensive future research. Recently, Westaway and Younger (2013) corrected the heat flow data base in Britain.

Correction for Recent Warming

Earth's climate has changed throughout history and the current warming trend is of particular significance. This warming has been predicted to be largely a result of the increase in CO_2 in the atmosphere, and the warming increases with latitude.

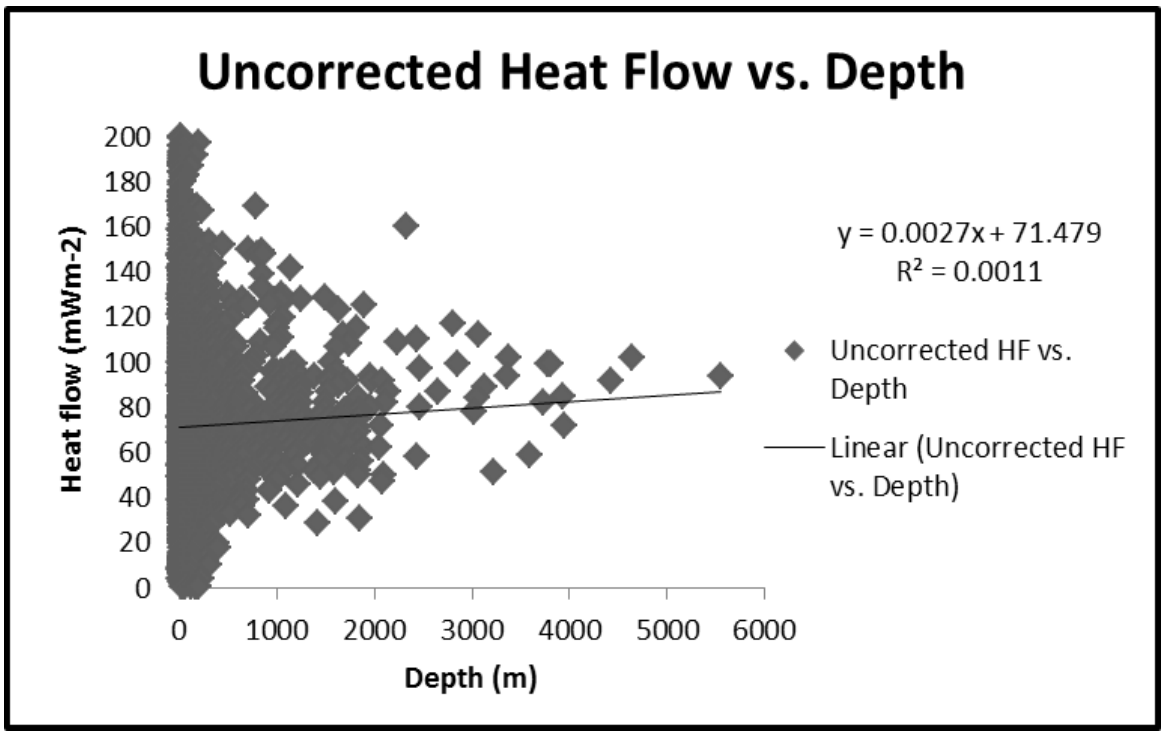

Figure 5. Uncorrected heat flow values in the United States versus depth of measurement. (Data source: SMU-UND United States Heat flow Database 2013)

Thus, a correction scheme based on latitude was developed to determine the effect of recent warming on temperature gradients measured in the upper few hundreds of meters in boreholes across the United States. The mean annual statewide temperatures for the period 1895-2012 along a north-south transect were gathered from the National Climatic Data Center.

Figure 6, shows the chart of temperature anomalies of the north-south transect of the central, east-central and west-central of the United States having a warming of +0.005^{o}C at 32.5^{o}N to 2.73^{o}C at 47.5^{o}N, +0.96^{o}C at 38.5^{o}N to 1.55^{o}C at 47.5^{o}N, and +0.18^{o}C at 35.5^{o}N to 1.52^{o}C at 47.5^{o}N, respectively based on their linear regression. Warming from a least square fit to the data shows an increase with latitude.

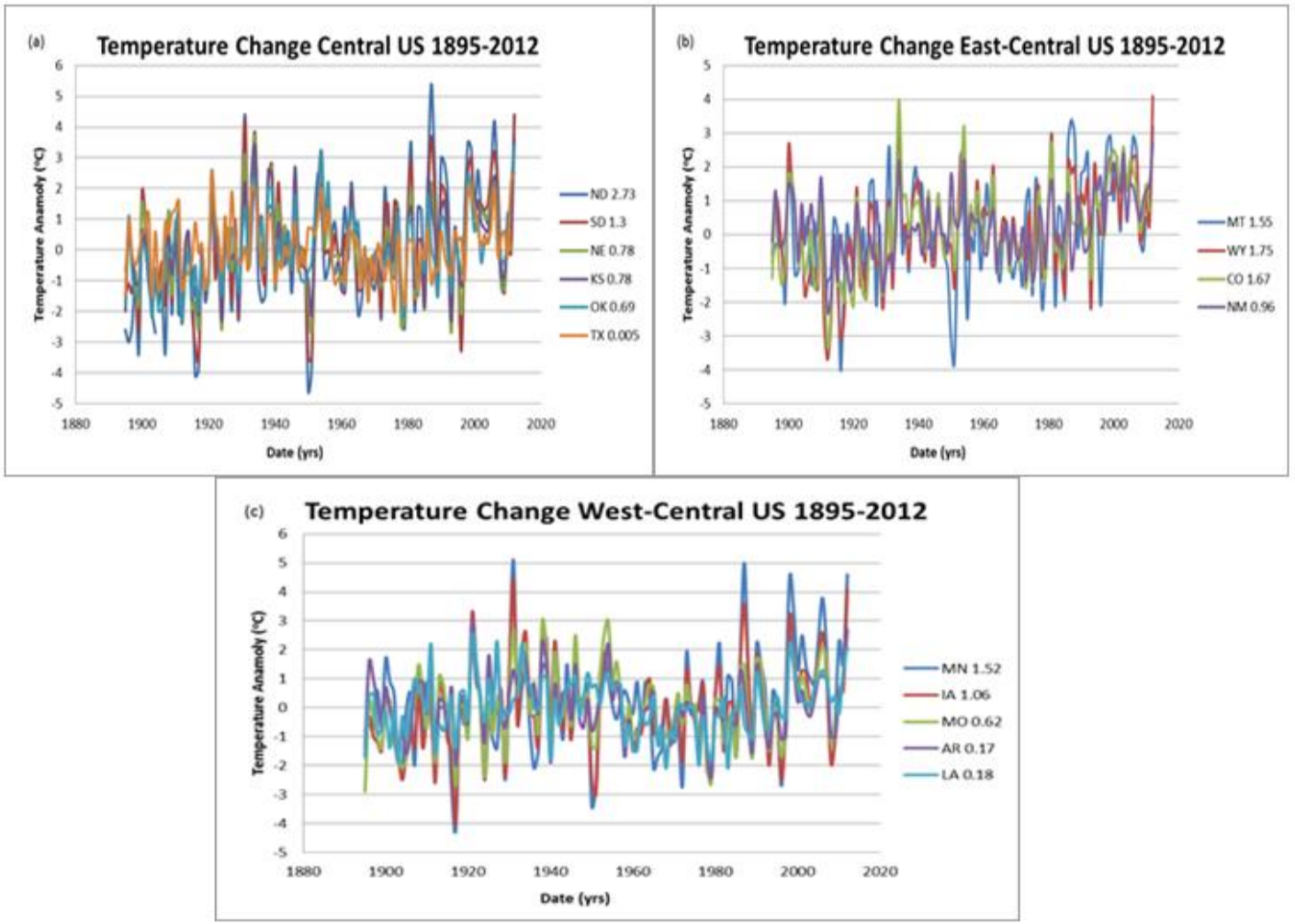

Figure 6. Chart showing mean annual statewide temperatures for the period 1895-2012 along a north-south transect from (a) ND TO TX (b) MT to NM (c) MN to LA. (Data Source: National Oceanic and Atmospheric Administration

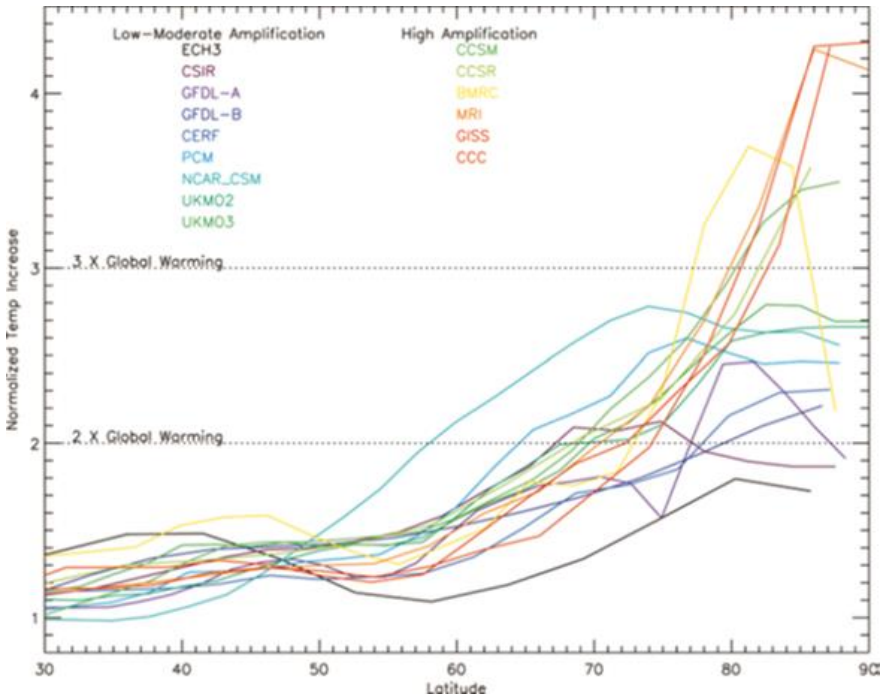

Figure 7. Chart showing the increase in zonal average 2-m air temperature for $2xCO_2$ conditions as function of latitude normalized by globally averaged air temperature increase. (Source: Holland & Bitz, 2003).

Comparing the results from the least squares fit to the chart in Figure 7 of Holland and Bitz (2003) affirms the result that warming signal increases with latitude. A trend line was fit to each north-south transect and equations in Table 1 can be used for correcting recent warming in the United States where x is Latitude (deg) and y is the Recent Warming Temperature (^{o}C) to be subtracted from temperature measured. This correction scheme being a function of latitude shows that warming has increased systematically with latitude from +0.7 ^{o}C at 41.6^{o}N to +2.3 ^{o}C at 49^{o}N and from +0.4 ^{o}C at 41.1^{o}N to +2.0 ^{o}C at 49.6^{o}N during the last century (Gosnold et al., 1997).

Table 1. Equations for Correcting Recent Warming in the United States.

North-South Transect	Equation
Central	$y = 0.1472x - 4.8401$
East-Central	$y = 0.0617x - 1.1692$
West-Central	$y = 0.119x - 4.2285$

x = Latitude (deg) and y = Recent Warming Temperature (^{o}C) to be subtracted from temperature measured.

Correction for Post-Glacial Warming

Temperature-depth profiles have been influenced by post-glacial warming and it accounts for underestimation of heat flow values (Hotchkiss & Ingersoll, 1934). These warming signals were initially considered to have had a minimal effect on the gradients (Birch, 1948) and were later concluded to have a larger effect (Jessop, 1971). Jessop stressed the importance of the correction that needs to be made within areas affected by the palaeoclimate, particularly the Canadian Shield.

Recent estimates of cold surface temperature during the Last Glacial Maximum shows that warming signal within North America has been underestimated. Blackwell and Richards (2004), in their Geothermal Map of North America, showed an area of low heat flow that was similar with the center of ice accumulation. During the Pleistocene, a post-glacial warming signal, which is a residue of a cold ice-free period, is accounted for by the heat flow patterns. Rolandone et al. (2003) interpreted that the ice base temperature was close to the pressure melting point. Analysis of some temperature-depth measurements with the northern hemisphere indicate that surface temperatures during the

LGM were colder than the melting point of ice and were of the order of -7^{o}C to -10^{o}C, implying that post-glacial warming may have been as much as 15^{o}C (Kukkonen & Joeleht, 2003; Gosnold et al., 2005). More so, temperature history recorded by pollen analysis in Manitoba (Ritchie, 1983) and surface temperature modeling (Ganopolski et al., 1997) asserts significant post-glacial warming of 15^{o}C.

Developed by Carslaw and Jaeger (1959), equation 2.1 is a depth related calculation used to model surface temperature variations. The concept is based on the fact that the warming disturbance at the surface propagating downward with depth is due to the diffusivity and conductivity character of the rock. In this study, a change in surface temperature T_0 of 15^{o}C, since the LGM of about 12 ka was used to model the effect of post-glacial warming signal and to estimate its effect on the gradient.

The effect of post-glacial warming on subsurface temperatures is greatest near the surface and diminishes with depth as shown in Figure 8. Figure 9 is based on the modeled 15^{o}C warming event at 12 ka and shows that heat flow values determined from depth less than 2000 m require corrections since the warming has disturbed the thermal gradient by 27%.

Applying the above correction to the heat flow values in the SMU-UND United States Heat Flow database, results in correction of the thermal gradient that has been underestimated at various depths where the heat flow value were measured. A comparison between Figure 5 and 10, shows clearly that the trend of heat flow increase with depth is related to paleoclimatic effect caused by ground surface temperature changes during the LGM.

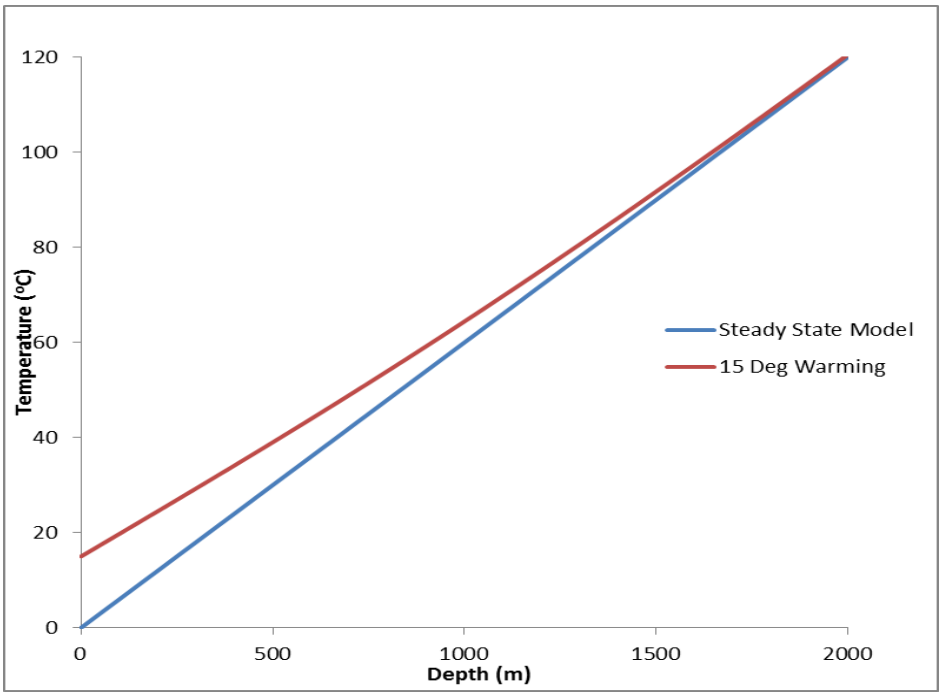

Figure 8. The effect of post-glacial warming on subsurface temperatures.

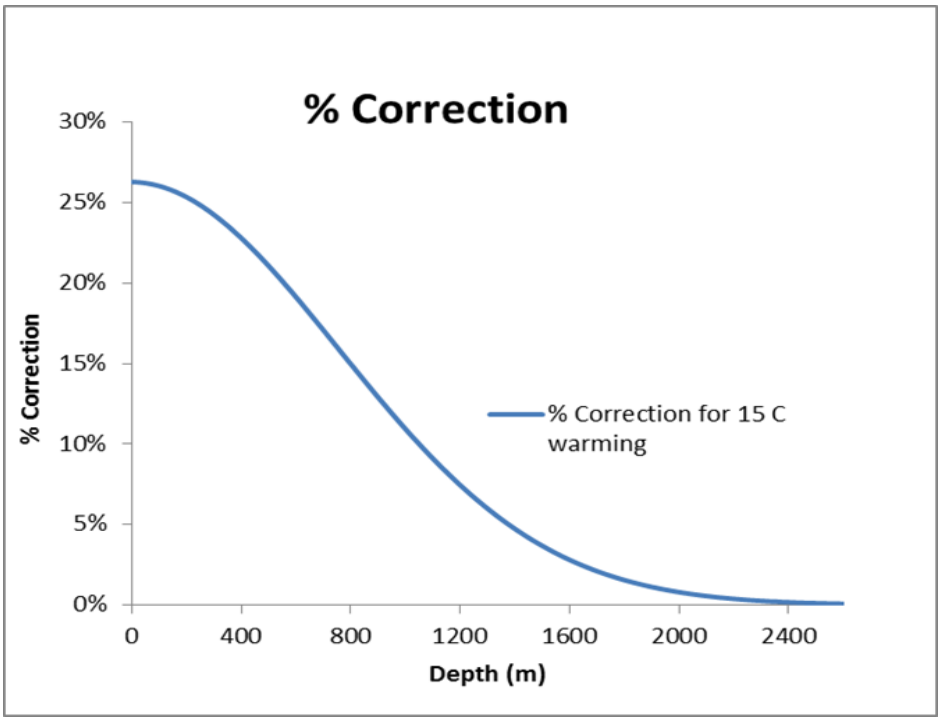

Figure 9. The modeled percentage change in heat flow with depth for 15°C warming event at 12 ka.

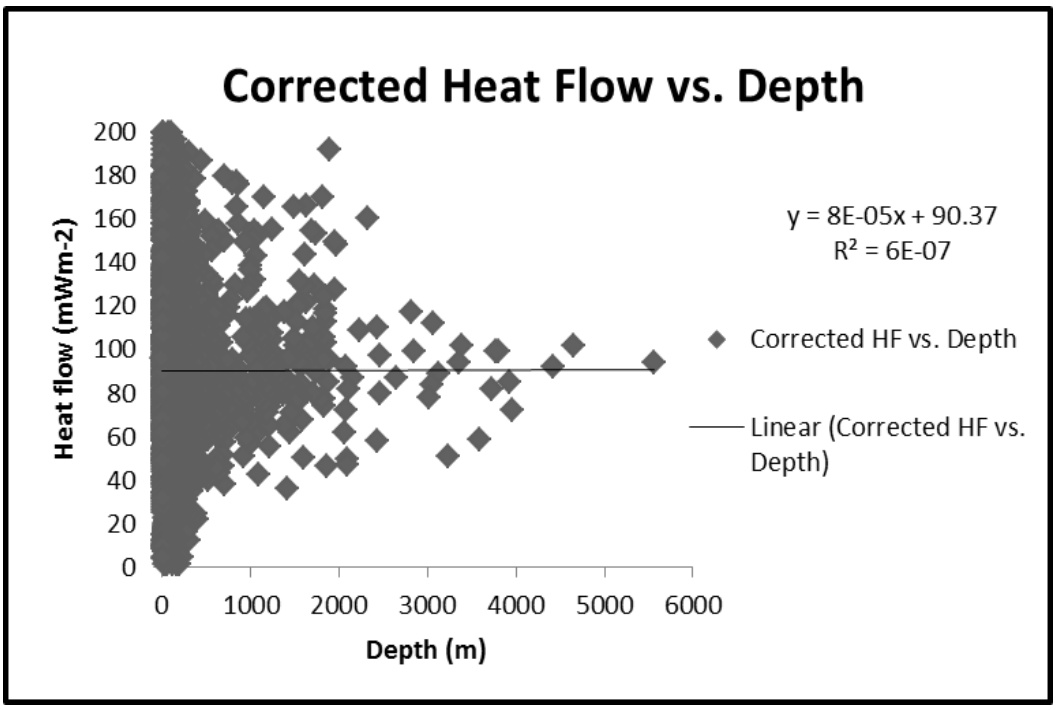

Figure 10. Corrected heat flow values in the United States versus depth of measurement. (Data source: SMU-UND United States Heat Flow Database 2013)

Heat Flow by Province

All measurements of heat flow in the United States lie within major physiographic and heat flow provinces as shown in Figure 4. In this study as seen in Table 1, averaging corrected heat flow values in the United States based on individual provinces will be valuable for geothermal studies. In this research a total of 2, 473 sites lie within the Western United States, and the provinces are often regions with high heat flow which is a result of thermal and tectonic activity associated with the Snake River Plain/Yellow Stone area. The Basin and Range, Columbia Basin and Northern Rocky Mountains are the largest provinces within the Western United States and they are also characterized by older volcanism. All these provinces including the Southern Rocky Mountains have a high average heat flow ranging from 78 – 96 mW m^{-2} as shown in Table 2. The Great

Plains province, except for areas affected by ground water movement, has a normal averaged heat flow of 75 mW m^{-2}.

Table 2. Mean Heat Flow Physiographical Provinces of the Western United States.

Provinces	Mean Heat Flow + SD (mW m^{-2})	Number of Data
Basin and Range	87 ± 32	649
Cascade-Sierra Mountains	67 ± 34	215
Colorado Plateau	71 ± 23	255
Columbia Plateau	78 ±42	744
Great Plains	75 ± 27	130
Lower Californian	67 ± 18	3
Middle Rocky Mountains	65 ± 21	26
Northern Rocky Mountains	84 ± 36	160
Pacific Border	45 ± 16	134
Southern Rocky Mountains	96 ± 33	126
Wyoming Basin	57 ± 11	31

The Eastern United States is generally characterized by low average heat flow based on 427 individual sites analyzed in this study as shown in Table 3. The Ozark and Appalachians Plateau have a high average heat flow ranging from 57 – 68 mW m^{-2}. The high heat flow in Ozark Plateau is associated with heat production in the basement rocks and may be related to regional ground water movement (Cranganu & Deming, 1998). The high heat flow in the Appalachians Plateau is a result of high crustal radioactivity.

Table 3. Mean Heat Flow Physiographical Provinces of the Eastern United States.

Provinces	Mean Heat Flow $\pm$ SD (mWm^{-2})	Number of Data
Adirondack	39 $\pm$ 7	5
Appalachian Plateau	57 $\pm$ 19	19
Blue Ridge	42 $\pm$ 10	11
Central Low Land	50 $\pm$ 13	78
Coastal Plain	51 $\pm$ 18	175
Interior Low Plateau	17	1
New England	56 $\pm$ 13	68
Ouachita	45 $\pm$ 0.5	2
Ozark Plateau	68 $\pm$ 25	5
Piedmont	45 $\pm$ 12	40
St Lawrence Valley	0	0
Superior Upland	43 $\pm$ 8	6
Valley and Ridge	49 $\pm$ 30	17

In this research, the Great Plains boundary was used as a demarcation between the Western and Eastern United States. From the analysis of 2, 900 heat flow data sites within the continental United States, results show that the average heat flow is 74 mW m^{-2}, 78 mW m^{-2} and 51 mW m^{-2} respectively for the whole conterminous United States, both Western and Eastern United States respectively as shown in Table 4.

Table 4. Summary of Average Heat Flow in the Whole Conterminous United States, Western and Eastern United States.

Segments	Mean Heat Flow $\pm$ SD (mW m^{-2})
Conterminous United States	58 $\pm$ 35
Western	78 $\pm$ 35
Eastern	51 $\pm$ 17

Conclusions

Heat flow measurements require correction for both recent warming and post-glacial warming signals. However, they have been underestimated in recent assessment of the United States heat flow data base.

This study determined that warming signals have increased systematically with latitude from +0.7 ^{o}C at 41.6^{o}N to +2.3 ^{o}C at 49^{o}N during the last century. This temperature increase agrees with the prediction that global warming due to increasing amount of CO_2 in the atmosphere varies with latitude.

A change in surface temperature T_0 of 15^{o}C, since the LGM occurred, applied for the correction of the heat flow values resulted in a corrected heat flow variation with depth, which was believed to be an effect of post-glacial warming. This result calls for

correction of all heat flow values determined from depths less than 2km since the warming disturbed the thermal gradient by 27%. Applying the correction to about 2, 900 heat flow data sites within the continental United States, shows that the average heat flow is 58 mW m^{-2}, 78 mW m^{-2} and 51 mW m^{-2} for the whole conterminous United States, Western and Eastern United States respectively.

The post-glacial warming corrections of heat flow values measured at shallow depth up to 2km at sites in the United States will lead to actual estimation of temperature at depth, enhanced geothermal energy systems, maturation of hydrocarbons and other related geophysical research.

APPENDICES

Appendix A
Physiographical Provinces of the United States

Western United States	Eastern United States
Basin and Range	Adirondack
Cascade-Sierra Mountains	Appalachian Plateau
Colorado Plateau	Blue Ridge
Columbia Plateau	Central Low Land
Great Plains	Coastal Plain
Lower Californian	Interior Low Plateau
Middle Rocky Mountains	New England
Northern Rocky Mountains	Ouachita
Pacific Border	Ozark Plateau
Southern Rocky Mountains	Piedmont
Wyoming Basin	St Lawrence Valley
	Superior Upland
	Valley and Ridge

Appendix B
Heat Flow Site Information

This appendix lists all heat flow well site information corrected in this study for post-glacial warming. The information include latitude, longitude, depth of measurement, temperature gradient, thermal conductivity, uncorrected heat flow value (UHF) and corrected heat flow value (CHF).

Table 5. Heat Flow Site Information.

Site #	Latitude	Longitude	Depth	Temp. Gradient	Conductivity	UHF	CHF
1	46.433	-119.780	900	37	1.59	59	59
2	36.367	-106.900	900	29	1.88	56	56
3	41.017	-111.530	888	21	2.8	64	64
4	38.884	-107.051	860	36	3.7	148	149
5	39.751	-105.834	854	35	3.84	133	134
6	38.885	-107.051	840	37	3.69	149	151
7	36.400	-107.420	823	27	2.8	68	69
8	37.683	-111.730	820	15	4.18	63	64
9	41.500	-103.100	800	55	1.09	60	61
10	38.884	-107.052	800	39	3.49	148	151
11	36.367	-106.900	800	38	1.97	76	77
12	36.367	-106.900	793	36	2.34	80	82
13	40.067	-109.350	762	25	2.18	53	54
14	36.550	-108.030	762	24	3.05	72	74
15	48.917	-102.430	760	56	1.13	61	63
16	33.283	-105.930	757	32	3.14	100	103
17	40.517	-112.150	750	0	2.97	61	63
18	32.017	-106.800	743	39	2.01	79	81
19	34.002	-107.800	732	57	1.21	71	73
20	33.100	-106.880	730	31	3.1	97	100
21	35.933	-107.470	716	30	2.34	71	73
22	38.885	-107.051	710	37	3.69	150	155
23	46.519	-122.800	710	18	1.76	32	33
24	39.752	-105.834	701	33	3.84	125	129
25	39.083	-94.167	701	16	2.89	48	50
26	41.201	-102.590	700	60	1.09	66	68
27	41.201	-102.590	700	60	1.09	66	68
28	46.518	-122.830	690	22	1.76	39	40
29	35.285	-119.535	685	31	1.67	52	54
30	36.817	-81.100	685	10	4.02	43	45
31	38.818	-109.700	677	14	5.9	86	89

Table 5. cont.

32	40.050	-108.333	671	66	0.92	62	64
33	39.967	-108.467	663	55	1.05	58	60
34	37.683	-111.730	660	29	2.18	63	66
35	40.533	-112.150	656	18	5.31	96	100
36	41.219	-107.230	650	10	3.65	36	37
37	48.917	-117.330	647	19	5.3	92	96
38	36.852	-116.300	643	41	3.1	128	133
39	35.867	-107.170	640	40	1.97	70	73
40	46.050	-112.550	640	30	2.85	87	91
41	29.800	-104.400	620	16	3.72	63	66
42	40.050	-108.333	617	56	1.09	62	65
43	33.250	-106.900	617	30	3.22	99	104
44	41.100	-74.584	613	13	2.89	39	41
45	37.283	-116.400	610	25	1.63	41	43
46	41.100	-74.584	610	12	2.97	38	40
47	46.350	-119.270	608	34	1.51	52	54
48	42.800	-78.850	608	0	0	50	52
49	44.585	-120.920	605	31	2.72	84	88
50	45.384	-121.800	600	51	1.84	96	101
51	35.850	-107.400	600	34	1.8	62	65
52	35.850	-107.400	600	34	0.59	62	65
53	34.617	-116.718	600	28	2.43	69	72
54	42.434	-89.851	600	23	3.31	75	79
55	36.700	-105.520	590	21	3.39	72	76
56	44.350	-103.750	584	19	4.48	82	86
57	38.917	-107.117	580	32	3.31	107	112
58	40.533	-112.150	576	18	5.52	96	101
59	32.768	-111.985	570	28	3.85	109	115
60	36.850	-108.530	564	59	1.13	63	66
61	36.767	-116.120	564	41	1.84	75	79
62	45.318	-121.700	560	67	1.76	120	126
63	37.783	-108.850	560	39	3.14	125	132
64	29.800	-104.400	560	21	3.81	80	84
65	34.650	-77.317	558	18	2.72	51	54
66	36.850	-76.469	557	22	3.47	79	83
67	32.319	-112.869	550	30	2.76	86	91
68	36.733	-108.280	550	27	2.72	76	80
69	39.983	-109.600	541	32	2.05	62	66
70	36.983	-94.867	540	21	2.64	56	59
71	46.352	-119.270	530	42	1.59	66	70
72	33.417	-106.950	520	32	2.76	89	94
73	47.817	-91.717	520	18	1.84	33	35

Table 5. cont.

74	39.002	-95.469	520	17	2.76	48	51
75	48.917	-117.330	518	22	5.09	101	107
76	38.150	-91.250	518	14	3.51	51	54
77	36.700	-105.530	510	21	3.39	72	76
78	44.850	-121.820	500	79	1.38	110	117
79	43.034	-115.451	500	70	1.46	102	108
80	41.550	-103.140	500	52	1.09	57	61
81	41.768	-103.700	500	46	1.09	50	53
82	36.833	-107.920	500	39	1.63	66	70
83	32.450	-106.600	500	35	2.89	103	109
84	35.650	-108.520	500	22	2.93	66	70
85	36.983	-94.867	500	19	3.14	61	65
86	35.267	-103.850	500	18	3.18	57	61
87	42.301	-106.780	500	14	3.77	54	57
88	32.200	-108.080	498	19	4.14	49	52
89	33.183	-106.880	495	32	2.89	92	98
90	39.568	-105.802	490	29	4.77	130	138
91	34.550	-117.717	488	24	2.76	69	73
92	39.433	-106.133	480	33	3.47	117	125
93	32.952	-109.618	480	32	2.51	83	88
94	31.833	-110.750	480	24	3.43	86	92
95	32.302	-112.853	480	24	3.72	90	96
96	36.283	-92.917	480	20	5.82	117	125
97	38.233	-79.817	480	14	3.51	50	53
98	31.134	-81.535	478	19	2.01	39	42
99	35.950	-107.900	473	29	2.3	64	68
100	36.600	-107.420	460	29	1.92	56	60
101	38.818	-109.700	457	13	6.07	80	85
102	37.350	-116.570	457	0	1.38	62	66
103	43.484	-112.683	455	41	1.55	65	69
104	36.700	-105.520	450	22	3.22	73	78
105	36.050	-92.867	450	13	5.19	67	72
106	39.433	-123.733	444	65	1.67	83	89
107	34.518	-77.451	444	33	0.96	33	35
108	39.367	-106.183	442	40	3.76	152	162
109	36.700	-105.470	440	26	3.22	87	93
110	39.517	-106.650	440	24	4.14	99	106
111	37.933	-106.950	430	35	2.81	100	107
112	34.250	-117.317	430	26	2.55	68	73
113	36.700	-105.530	430	23	3.22	75	80
114	38.818	-109.700	430	16	3.77	62	66
115	34.002	-107.800	427	48	1.34	66	71

Table 5. cont.

116	38.152	-109.600	427	21	2.8	61	65
117	43.867	-111.751	425	44	1.76	79	85
118	36.367	-106.900	420	32	1.97	63	67
119	48.051	-118.700	420	23	2.97	69	74
120	33.267	-86.017	420	14	2.72	39	42
121	40.050	-108.517	411	60	1.17	83	89
122	37.383	-108.067	410	30	2.89	87	93
123	32.534	-108.367	410	23	3.76	86	92
124	43.083	-79.000	410	0	0	48	51
125	43.753	-112.684	407	59	1.84	110	118
126	39.967	-108.467	404	54	1.05	58	62
127	38.967	-116.630	401	51	1.63	83	89
128	41.217	-103.050	400	50	1.09	55	59
129	41.217	-103.050	400	50	1.09	55	59
130	42.317	-117.900	400	40	1.72	70	75
131	39.318	-106.119	400	37	3.21	113	121
132	38.968	-106.434	400	35	3.39	119	128
133	39.267	-114.980	400	29	2.55	76	82
134	44.217	-73.533	400	18	1.92	33	35
135	34.819	-98.434	400	15	2.93	47	50
136	43.167	-95.183	400	8	2.22	18	19
137	46.733	-89.567	396	17	2.47	44	47
138	36.600	-115.780	396	15	5.94	90	97
139	46.519	-122.830	395	24	1.46	35	38
140	32.200	-108.080	391	17	3.31	57	61
141	44.300	-103.670	383	9	2.13	20	22
142	36.900	-108.020	380	35	1.88	67	72
143	35.850	-107.400	380	32	1.88	61	66
144	36.750	-107.720	380	29	2.01	59	63
145	38.500	-105.333	380	25	3.14	76	82
146	46.535	-122.840	375	25	1.46	36	39
147	36.917	-104.870	370	38	2.64	102	110
148	32.386	-111.386	370	37	2.55	94	101
149	31.883	-111.000	370	28	3.56	103	111
150	35.300	-106.170	370	22	2.64	58	62
151	39.850	-104.850	368	36	2.43	89	96
152	36.417	-108.030	366	37	2.47	70	75
153	34.550	-117.717	366	24	2.89	69	74
154	33.283	-81.667	364	15	2.89	44	47
155	34.650	-77.317	363	37	1.46	55	59
156	38.433	-75.051	363	26	1.26	34	37
157	40.386	-105.968	360	43	3.67	144	155

Table 5. cont.

158	33.050	-108.500	360	40	2.64	107	115
159	43.200	-78.467	352	0	0	49	53
160	34.534	-80.736	351	14	3.05	45	49
161	37.267	-105.233	350	58	1.72	101	109
162	43.084	-104.020	350	54	1.09	58	63
163	42.317	-117.900	350	38	1.72	66	71
164	34.800	-107.130	350	35	2.26	82	88
165	48.917	-117.330	350	26	5.15	115	124
166	48.917	-117.330	350	23	5.15	118	127
167	43.283	-72.817	350	19	2.64	51	55
168	33.867	-115.433	350	19	2.72	53	57
169	42.818	-105.300	340	44	2.05	89	96
170	42.818	-105.300	340	44	2.05	89	96
171	46.518	-122.830	340	24	1.46	36	39
172	33.083	-109.367	340	22	2.89	64	69
173	34.750	-112.069	340	18	3.6	66	71
174	35.533	-106.980	335	39	1.8	71	77
175	41.100	-74.584	335	12	2.89	36	39
176	45.318	-121.700	330	71	1.55	111	120
177	40.136	-101.470	330	53	1.09	58	63
178	36.533	-106.850	330	37	1.8	67	72
179	31.983	-111.067	330	37	3.26	124	134
180	37.733	-117.180	330	26	3.64	96	104
181	36.700	-105.470	330	24	3.43	83	90
182	33.733	-106.030	330	20	2.89	60	65
183	31.450	-104.880	330	15	2.85	41	44
184	38.233	-79.817	330	15	3.01	46	50
185	36.519	-76.868	328	23	2.59	60	65
186	48.917	-117.330	327	18	4.77	87	94
187	32.403	-103.740	322	78	5.73	44	48
188	31.934	-110.685	320	27	2.51	68	74
189	37.200	-82.100	320	26	2.18	58	63
190	35.551	-90.034	320	22	2.72	60	65
191	48.917	-117.330	320	22	4.81	96	104
192	32.017	-105.480	320	21	4.02	84	91
193	34.919	-118.801	320	19	2.89	55	59
194	46.450	-113.420	320	18	4.31	79	85
195	34.934	-118.802	320	18	2.89	53	57
196	38.233	-79.817	320	13	4.06	52	56
197	45.319	-121.650	310	79	1.92	153	166
198	32.450	-106.600	310	36	3.68	135	146
199	47.367	-120.300	310	28	2.18	61	66

Table 5. cont.

200	36.700	-105.530	310	20	3.85	78	84
201	35.250	-106.180	310	19	2.59	52	56
202	36.700	-105.520	310	18	3.85	71	77
203	34.567	-78.933	307	19	2.93	58	63
204	40.983	-80.133	305	28	1.76	50	54
205	42.767	-109.570	305	19	3.01	57	62
206	34.769	-83.268	305	19	2.8	54	58
207	42.767	-109.570	305	18	2.93	50	54
208	35.917	-84.317	305	11	2.55	30	32
209	47.234	-124.180	304	27	1.3	35	38
210	36.951	-76.267	301	24	1.88	47	51
211	45.417	-121.770	300	77	1.72	134	145
212	44.535	-121.950	300	69	1.34	94	102
213	39.717	-113.220	300	55	2.26	125	135
214	38.168	-75.568	300	52	1.13	59	64
215	42.317	-117.900	300	49	1.72	83	90
216	35.667	-108.130	300	47	1.97	92	100
217	32.400	-106.120	300	42	3.05	128	139
218	38.983	-106.451	300	41	3.01	115	125
219	38.900	-107.102	300	40	3.3	129	140
220	36.533	-106.480	300	39	2.01	79	86
221	38.984	-106.935	300	37	3.59	108	117
222	37.800	-107.617	300	36	2.47	91	99
223	48.368	-101.450	300	36	1.17	43	47
224	39.500	-105.917	300	31	3.18	99	107
225	39.568	-105.803	300	30	3.55	96	104
226	35.867	-106.150	300	30	2.3	69	75
227	38.917	-107.117	300	29	3.18	93	101
228	31.369	-110.684	300	28	3.51	99	107
229	36.367	-106.900	300	27	1.97	54	58
230	30.702	-87.001	300	27	1.46	41	44
231	39.018	-107.084	300	26	3.54	96	104
232	34.250	-117.319	300	25	2.64	66	71
233	35.367	-114.134	300	24	2.97	73	79
234	36.269	-76.201	300	23	1.46	35	38
235	37.569	-107.585	300	22	3.63	88	95
236	34.885	-111.834	300	14	3.22	46	50
237	43.484	-112.683	300	5	1.97	10	11
238	40.517	-112.150	300	0	4.77	79	86
239	36.318	-76.051	299	27	1.76	48	52
240	38.335	-75.601	297	47	1.21	59	64
241	38.168	-75.369	297	40	1.3	53	57

Table 5. cont.

242	36.901	-76.700	297	26	2.18	59	64
243	38.069	-75.718	296	48	1.26	61	66
244	35.517	-75.984	296	23	2.05	48	52
245	37.935	-75.451	296	19	1.92	37	40
246	37.285	-75.919	295	66	0.88	59	64
247	38.384	-75.684	295	45	1.09	51	55
248	36.850	-76.469	295	34	2.43	83	90
249	38.034	-75.667	293	46	1.34	63	68
250	36.800	-76.035	293	33	1.3	44	48
251	40.302	-74.050	292	22	2.26	51	55
252	33.434	-81.234	292	21	3.26	70	76
253	34.567	-78.933	291	22	2.76	62	67
254	42.817	-116.153	290	70	1.88	131	142
255	32.953	-109.602	290	34	2.22	74	80
256	37.533	-104.900	290	34	2.43	83	90
257	35.217	-107.320	290	30	2.55	79	86
258	32.200	-108.080	290	23	2.72	64	69
259	33.733	-106.030	290	22	2.05	46	50
260	48.903	-117.590	290	20	6.02	122	132
261	37.319	-95.201	290	14	4.44	61	66
262	34.919	-111.818	290	12	3.68	44	48
263	38.769	-75.619	289	51	0.96	51	55
264	38.433	-75.051	289	36	2.01	74	80
265	36.901	-76.700	287	21	2.26	49	53
266	45.302	-112.870	285	21	2.59	54	59
267	38.034	-77.885	284	16	2.26	37	40
268	42.134	-122.720	283	16	3.01	41	44
269	38.717	-116.030	282	34	1.8	62	67
270	32.752	-110.369	280	64	2.01	130	141
271	39.950	-108.383	280	56	0.84	44	48
272	36.617	-108.620	280	52	1.84	96	104
273	35.667	-75.750	280	35	1.88	68	74
274	40.119	-105.384	280	32	2.47	100	108
275	35.333	-107.620	280	32	2.26	73	79
276	36.600	-107.350	280	30	1.92	58	63
277	36.717	-105.400	280	29	2.85	78	85
278	32.335	-112.902	280	26	2.85	79	86
279	48.219	-115.902	280	19	3.72	73	79
280	38.850	-119.750	280	19	2.43	47	51
281	37.100	-119.733	280	8	2.93	25	27
282	37.901	-79.886	279	9	5.19	48	52
283	37.034	-76.302	278	30	1.92	58	63

Table 5. cont.

284	36.718	-121.401	278	26	2.76	71	77
285	35.533	-106.980	277	18	2.26	41	44
286	45.319	-121.650	275	68	2.01	138	150
287	45.319	-121.650	275	51	2.01	91	99
288	34.233	-107.630	274	43	1.8	79	86
289	34.283	-113.935	274	34	2.13	70	76
290	32.884	-80.351	274	27	1.97	54	59
291	34.734	-117.768	274	23	2.47	64	69
292	42.450	-78.633	274	0	0	49	53
293	36.617	-108.620	270	52	1.84	96	104
294	41.769	-101.670	270	47	1.17	56	61
295	36.800	-104.950	270	37	2.13	79	86
296	39.285	-106.469	270	36	4.07	138	150
297	32.500	-106.100	270	32	2.09	68	74
298	36.533	-106.850	270	32	2.05	66	72
299	38.683	-106.500	270	27	2.76	77	84
300	34.769	-83.268	270	27	1.97	53	58
301	33.153	-110.819	270	25	2.97	73	79
302	38.783	-106.167	260	39	2.05	82	89
303	39.285	-106.468	260	36	3.33	107	116
304	33.133	-109.917	260	32	2.38	79	86
305	38.950	-118.630	260	32	2.43	78	85
306	30.583	-87.117	260	30	2.01	62	67
307	46.235	-112.430	260	26	3.1	82	89
308	32.100	-110.051	260	26	2.8	74	80
309	36.750	-107.720	260	26	1.84	50	54
310	34.783	-108.270	260	25	3.97	101	110
311	46.534	-122.820	260	21	1.46	31	34
312	43.117	-70.917	260	17	2.64	45	49
313	44.583	-73.900	260	15	3.31	51	55
314	39.667	-79.983	260	9	5.19	46	50
315	40.550	-117.100	259	31	4.69	146	159
316	34.219	-77.852	257	26	1.55	41	45
317	38.917	-77.100	256	16	2.93	46	50
318	39.317	-76.767	254	15	3.18	49	53
319	38.383	-98.167	252	13	5.23	69	75
320	37.034	-76.302	251	27	1.92	53	58
321	43.250	-100.190	250	93	1.21	111	121
322	37.267	-105.233	250	64	1.67	108	117
323	42.317	-117.900	250	58	1.72	100	109
324	48.934	-100.820	250	54	1.13	60	65
325	31.801	-111.301	250	51	1.92	98	107

Table 5. cont.

326	35.217	-107.320	250	45	2.51	115	125
327	41.169	-103.670	250	41	1.09	45	49
328	41.169	-103.670	250	41	1.09	45	49
329	40.401	-105.951	250	37	4.07	138	150
330	35.850	-108.050	250	35	2.05	66	72
331	34.434	-112.486	250	28	2.97	84	91
332	37.400	-118.000	250	28	2.76	75	82
333	39.067	-114.920	250	26	3.31	85	92
334	43.135	-113.235	250	15	1.38	20	22
335	38.233	-79.817	250	14	3.47	48	52
336	38.867	-120.650	250	11	3.68	44	48
337	45.301	-121.670	250	10	2.34	24	26
338	38.833	-121.167	250	9	2.89	25	27
339	37.200	-82.100	250	9	5.94	54	59
340	34.567	-78.933	249	21	3.26	69	75
341	39.400	-120.868	246	7	4.35	28	30
342	34.635	-113.968	244	39	2.43	91	99
343	34.151	-113.168	244	35	1.92	67	73
344	35.867	-107.170	244	30	2.34	72	78
345	34.550	-117.717	244	24	2.93	69	75
346	37.650	-91.167	244	16	3.26	54	59
347	38.917	-77.100	244	15	3.1	46	50
348	40.367	-75.833	243	10	2.8	29	32
349	34.967	-108.750	240	71	1.67	122	133
350	40.150	-100.150	240	51	1.09	56	61
351	40.201	-101.150	240	51	1.09	56	61
352	41.652	-101.470	240	49	1.09	53	58
353	32.900	-109.030	240	41	2.8	115	125
354	32.533	-106.420	240	39	2.3	91	99
355	32.352	-89.500	240	27	1.55	43	47
356	40.401	-105.934	240	26	3.82	90	98
357	38.983	-106.518	240	25	3.39	100	109
358	43.933	-71.533	240	25	3.51	89	97
359	48.601	-120.380	240	23	3.18	73	79
360	48.451	-101.320	235	40	1.17	48	52
361	38.367	-98.167	235	12	4.98	62	67
362	38.168	-75.369	234	33	1.34	45	49
363	38.319	-75.502	233	31	1.46	46	50
364	39.102	-75.452	231	49	1.26	61	66
365	43.984	-117.220	230	114	1.46	167	182
366	44.067	-116.619	230	87	1.17	102	111
367	34.033	-107.220	230	44	2.76	124	135

Table 5. cont.

368	45.419	-121.280	230	41	1.59	65	71
369	36.700	-107.720	230	28	1.88	55	60
370	36.400	-104.230	230	27	2.43	67	73
371	35.333	-106.180	230	27	2.55	71	77
372	32.134	-110.068	230	24	3.26	78	85
373	40.302	-74.050	230	20	1.59	33	36
374	35.533	-106.980	229	10	2.38	25	27
375	40.567	-75.200	229	10	3.43	37	40
376	36.384	-78.967	229	10	3.81	41	45
377	38.917	-116.330	228	38	1.55	58	63
378	38.917	-77.100	228	16	2.89	46	50
379	47.050	-114.284	227	21	3.43	74	81
380	40.536	-124.168	227	0	0	54	59
381	38.034	-75.667	226	38	1.13	43	47
382	38.335	-75.601	226	37	1.67	63	69
383	46.168	-108.600	225	25	1.67	42	46
384	39.518	-94.818	225	22	2.8	61	66
385	32.800	-108.070	225	22	3.01	75	82
386	34.653	-83.168	225	18	2.8	53	58
387	38.386	-75.568	224	31	1.59	50	54
388	45.917	-120.180	224	17	1.59	43	47
389	39.834	-74.169	222	33	1.38	46	50
390	36.217	-104.680	220	53	2.3	123	134
391	38.984	-106.935	220	39	3.29	112	122
392	35.717	-114.367	220	39	2.97	117	127
393	32.635	-108.486	220	30	2.83	86	94
394	36.783	-107.830	220	29	2.47	71	77
395	41.233	-79.519	220	24	3.18	76	83
396	31.867	-110.800	220	24	3.1	74	81
397	45.917	-112.000	220	24	3.26	78	85
398	34.769	-83.268	220	23	1.92	46	50
399	38.468	-94.901	220	20	2.85	59	64
400	35.117	-107.770	220	19	2.93	57	62
401	37.719	-109.350	220	17	3.89	67	73
402	39.700	-122.800	220	16	2.93	48	52
403	45.302	-112.870	220	13	4.81	67	73
404	43.300	-73.617	220	9	4.6	43	47
405	46.451	-120.220	215	31	1.59	49	53
406	38.384	-75.684	213	52	1	53	58
407	38.069	-75.718	213	48	1.3	64	70
408	37.050	-116.000	213	42	0.75	32	35
409	38.168	-75.568	212	52	0.96	51	56

Table 5. cont.

410	37.285	-75.919	211	44	1.34	59	64
411	35.902	-82.118	211	16	2.68	45	49
412	35.217	-107.320	210	50	2.8	143	156
413	43.918	-109.280	210	35	2.65	74	81
414	36.600	-107.350	210	32	1.63	53	58
415	43.467	-116.068	210	31	2.51	78	85
416	39.902	-105.586	210	30	2.38	71	77
417	34.635	-113.683	210	28	2.75	77	84
418	34.868	-118.750	210	26	3.51	92	100
419	42.617	-72.450	210	25	2.76	69	75
420	38.167	-104.783	210	23	4.52	105	114
421	39.018	-107.085	210	23	4.27	100	109
422	44.468	-113.284	210	22	2.59	58	63
423	32.035	-110.067	210	21	3.01	66	72
424	44.233	-73.467	210	18	1.88	33	36
425	37.719	-109.350	210	17	3.89	67	73
426	37.951	-75.585	209	49	1.3	65	71
427	44.483	-113.268	207	83	1.26	105	114
428	35.517	-75.984	207	49	1.13	55	60
429	45.767	-122.190	205	24	2.8	68	74
430	48.352	-118.870	205	22	3.1	69	75
431	46.350	-122.100	205	18	3.85	69	75
432	44.367	-103.880	204	26	3.05	79	86
433	37.167	-120.067	203	6	2.97	18	20
434	46.083	-97.083	202	19	2.59	50	55
435	39.767	-108.150	201	55	1.09	62	68
436	37.100	-119.383	201	12	2.55	32	35
437	33.567	-107.600	200	81	2.38	197	215
438	42.234	-113.367	200	54	2.09	112	122
439	41.601	-101.800	200	54	1.17	64	70
440	45.769	-103.620	200	52	1.09	58	63
441	34.967	-108.750	200	50	2.43	124	135
442	45.769	-103.650	200	46	1.09	51	56
443	34.083	-107.370	200	44	1.72	92	100
444	38.885	-107.050	200	42	3.25	150	164
445	44.033	-115.783	200	41	2.8	115	125
446	32.983	-109.783	200	37	2.05	75	82
447	32.783	-111.483	200	35	1.55	54	59
448	32.100	-112.750	200	34	2.89	101	110
449	40.118	-100.170	200	33	1.09	36	39
450	46.367	-116.950	200	33	1.72	58	63
451	42.568	-76.951	200	32	2.01	64	70

Table 5. cont.

452	40.252	-96.183	200	32	3.26	105	114
453	37.601	-107.602	200	31	3.68	102	111
454	34.783	-108.270	200	31	3.31	105	114
455	46.967	-110.702	200	30	3.31	99	108
456	34.283	-107.250	200	29	2.47	71	77
457	38.083	-114.620	200	26	2.93	78	85
458	39.902	-105.601	200	25	2.42	63	69
459	30.617	-84.634	200	24	1.38	35	38
460	34.585	-113.185	200	22	2.97	66	72
461	42.817	-71.750	200	22	3.43	77	84
462	43.267	-71.983	200	22	2.93	66	72
463	39.000	-106.501	200	21	3.51	88	96
464	43.200	-71.533	200	20	3.56	72	78
465	34.268	-117.319	200	18	2.47	45	49
466	37.500	-90.667	200	16	3.22	51	56
467	41.750	-70.083	200	15	3.14	48	52
468	41.200	-107.020	200	12	3.14	36	39
469	43.833	-85.583	200	0	0	50	55
470	45.751	-121.540	199	21	1.59	34	37
471	34.233	-107.630	198	43	1.8	79	86
472	38.567	-116.930	198	25	3.01	74	81
473	38.818	-109.700	198	13	6.15	84	92
474	35.750	-75.785	196	63	1.59	102	111
475	36.601	-76.001	196	44	1.3	56	61
476	44.119	-116.636	195	67	1.17	78	85
477	46.268	-114.070	195	51	1.55	80	87
478	38.583	-116.200	192	31	1.8	53	58
479	34.768	-76.652	192	31	1.38	43	47
480	45.834	-122.520	192	25	1.59	40	44
481	35.784	-78.417	192	18	2.97	55	60
482	45.384	-121.800	190	65	1.55	100	109
483	36.533	-106.850	190	58	1.97	115	125
484	35.883	-106.150	190	33	2.13	72	79
485	38.300	-104.767	190	30	4.48	135	147
486	33.386	-110.853	190	28	4.23	117	128
487	43.701	-115.684	190	25	3.6	78	85
488	37.200	-82.100	190	24	2.18	53	58
489	32.533	-106.420	190	23	2.3	53	58
490	35.250	-106.180	190	22	2.59	59	64
491	36.467	-103.600	190	20	3.31	54	59
492	36.700	-105.520	190	19	3.05	58	63
493	36.819	-77.317	190	18	2.72	51	56

Table 5. cont.

494	44.119	-111.768	190	17	1.46	25	27
495	34.653	-83.168	189	20	2.09	43	47
496	34.751	-83.235	189	19	2.76	53	58
497	37.335	-80.767	188	21	6.19	131	143
498	38.486	-75.086	187	19	1.63	32	35
499	36.035	-110.518	185	15	1.67	61	67
500	37.917	-106.950	183	41	2.66	119	130
501	37.683	-118.533	183	33	2.51	83	91
502	32.668	-108.480	183	28	3.14	90	98
503	38.152	-109.600	183	23	3.01	71	77
504	33.917	-82.117	182	17	3.81	67	73
505	37.633	-115.550	182	13	3.39	45	49
506	36.800	-76.035	181	46	1.3	59	64
507	36.800	-76.035	181	40	1.3	52	57
508	35.217	-107.020	180	75	2.22	169	184
509	44.317	-111.451	180	65	1.88	108	118
510	45.269	-121.730	180	53	1.76	94	103
511	32.800	-108.070	180	48	1.59	83	91
512	32.101	-90.618	180	45	1.26	58	63
513	37.935	-75.451	180	45	1.51	69	75
514	33.283	-107.720	180	43	2.22	98	107
515	32.967	-107.530	180	32	2.3	74	81
516	35.467	-115.130	180	27	3.56	97	106
517	35.667	-108.130	180	27	2.38	66	72
518	34.684	-118.434	180	24	2.64	65	71
519	29.800	-104.400	180	24	3.43	86	94
520	36.700	-105.470	180	22	3.31	75	82
521	32.617	-110.801	180	22	3.43	77	84
522	47.451	-116.067	180	21	3.6	79	86
523	35.250	-106.180	180	21	2.59	56	61
524	36.617	-108.620	180	20	2.09	44	48
525	36.600	-110.150	180	19	3.97	71	77
526	42.451	-106.050	180	18	4.03	74	81
527	38.833	-120.250	180	11	2.97	34	37
528	38.735	-75.452	176	31	1.38	44	48
529	37.884	-75.500	175	41	1.63	68	74
530	34.734	-117.768	175	23	2.68	64	70
531	39.700	-122.883	175	15	4.31	66	72
532	44.383	-111.250	175	12	1.88	25	27
533	46.350	-119.270	174	30	1.59	47	51
534	35.234	-77.585	174	27	2.55	71	78
535	46.350	-119.270	174	25	1.63	41	45

Table 5. cont.

536	35.851	-78.469	174	16	2.89	49	53
537	36.318	-76.051	172	44	1.17	52	57
538	37.717	-117.780	172	36	2.22	81	88
539	33.535	-83.102	172	19	3.35	64	70
540	45.368	-109.900	171	20	3.01	61	67
541	43.919	-117.200	170	98	1.17	112	122
542	36.183	-104.670	170	64	2.09	136	148
543	46.869	-118.920	170	57	1.59	91	99
544	46.400	-116.918	170	46	1.72	79	86
545	34.150	-107.300	170	40	1.97	79	86
546	35.300	-106.250	170	36	2.3	84	92
547	33.053	-111.417	170	33	2.68	88	96
548	45.318	-122.870	170	30	1.59	47	51
549	35.700	-107.930	170	29	3.05	89	97
550	34.635	-113.684	170	28	2.8	80	87
551	46.952	-110.735	170	27	2.72	71	78
552	31.735	-109.785	170	27	3.64	98	107
553	37.783	-108.767	170	27	3.01	82	90
554	38.950	-108.617	170	26	2.22	58	63
555	36.033	-110.517	170	24	3.47	76	83
556	34.884	-118.768	170	24	3.47	84	92
557	36.617	-108.620	170	22	2.22	49	54
558	47.018	-112.369	170	19	4.69	92	100
559	32.533	-108.350	170	17	0.46	86	94
560	34.700	-80.452	170	12	3.1	40	44
561	38.684	-110.520	170	11	4.02	45	49
562	38.550	-120.567	170	10	3.01	30	33
563	41.467	-106.270	170	7	5.61	43	47
564	38.400	-76.184	168	55	1.05	58	63
565	47.283	-103.300	168	38	1.51	55	60
566	44.033	-71.483	168	25	3.68	94	103
567	33.033	-110.683	168	18	3.18	58	63
568	34.302	-81.135	166	18	3.35	61	67
569	40.401	-121.436	165	51	1.63	84	92
570	48.717	-119.580	165	21	3.47	75	82
571	42.286	-108.850	165	18	2.51	46	50
572	43.501	-112.934	165	8	1.38	11	12
573	36.951	-76.267	164	42	1.42	60	66
574	37.701	-75.702	164	32	2.05	66	72
575	47.001	-118.800	164	19	1.59	30	33
576	38.003	-75.818	163	61	1.09	68	74
577	45.367	-109.820	163	17	3.26	58	63

Table 5. cont.

578	42.786	-115.251	160	110	1.17	129	141
579	43.233	-116.285	160	84	1.17	98	107
580	39.752	-105.685	160	68	3.78	192	210
581	36.767	-105.970	160	64	1.76	115	126
582	37.450	-122.033	160	58	1.42	84	92
583	35.200	-107.020	160	55	2.09	116	127
584	36.883	-104.720	160	50	2.22	113	123
585	46.236	-119.400	160	43	1.59	68	74
586	30.583	-87.117	160	40	1.21	50	55
587	38.984	-106.935	160	39	3.41	105	115
588	45.735	-121.100	160	39	1.59	61	67
589	46.119	-116.990	160	36	1.59	57	62
590	37.800	-107.617	160	36	2.55	94	103
591	35.250	-107.220	160	32	2.72	88	96
592	45.534	-122.570	160	32	1.46	47	51
593	31.850	-108.300	160	32	3.47	112	122
594	39.233	-115.570	160	31	2.89	89	97
595	43.767	-112.519	160	28	1.84	51	56
596	31.736	-109.785	160	28	3.89	111	121
597	35.133	-113.817	160	26	3.35	89	97
598	33.485	-116.586	160	25	3.1	78	85
599	43.333	-72.550	160	21	2.3	50	55
600	43.250	-72.833	160	20	2.47	51	56
601	40.517	-120.669	160	19	2.43	46	50
602	39.035	-110.900	160	14	3.81	56	61
603	37.334	-118.534	160	14	2.68	38	42
604	42.383	-71.117	160	13	3.77	50	55
605	38.800	-75.185	159	26	1.63	43	47
606	40.385	-121.534	158	64	2.05	131	143
607	42.967	-113.451	155	24	1.34	32	35
608	38.967	-119.270	155	16	4.02	65	71
609	35.950	-78.319	155	16	2.93	49	54
610	38.817	-116.450	154	39	1.26	50	55
611	47.869	-117.270	154	24	2.76	68	74
612	39.567	-123.117	153	21	3.51	75	82
613	39.950	-112.050	152	79	1.97	154	168
614	47.167	-104.000	152	37	1.51	54	59
615	38.483	-113.130	152	32	2.8	92	101
616	32.183	-111.117	152	29	3.6	107	117
617	34.650	-116.683	152	20	3.26	66	72
618	37.333	-82.000	152	18	4.23	71	78
619	37.183	-116.200	152	16	4.9	79	86

Table 5. cont.

620	33.984	-115.684	152	14	2.85	39	43
621	44.901	-121.870	150	63	1.46	94	103
622	35.200	-107.080	150	60	2.22	133	145
623	38.683	-116.470	150	52	0.96	50	55
624	37.619	-119.068	150	51	3.05	156	170
625	42.784	-102.650	150	45	1.67	77	84
626	35.867	-106.150	150	40	2.22	89	97
627	46.519	-122.830	150	33	1.09	36	39
628	41.819	-121.250	150	33	1.97	66	72
629	34.033	-107.220	150	33	2.43	82	90
630	38.317	-117.300	150	32	3.22	105	115
631	48.653	-118.770	150	31	2.38	75	82
632	46.419	-120.170	150	28	1.59	43	47
633	34.650	-118.484	150	28	2.43	70	76
634	32.417	-111.533	150	28	3.43	98	107
635	30.917	-105.200	150	27	3.18	87	95
636	35.583	-105.250	150	27	2.3	62	68
637	35.267	-103.850	150	26	2.18	58	63
638	33.417	-110.951	150	25	3.51	89	97
639	45.768	-122.190	150	24	2.8	69	75
640	34.852	-118.735	150	24	3.47	84	92
641	38.950	-108.617	150	23	2.38	56	61
642	37.983	-109.050	150	23	2.68	61	67
643	44.050	-70.617	150	22	3.39	75	82
644	37.983	-109.050	150	22	2.68	61	67
645	38.433	-108.767	150	22	2.51	55	60
646	38.200	-108.817	150	21	2.68	57	62
647	44.100	-72.000	150	20	2.72	56	61
648	40.884	-86.467	150	19	3.01	58	63
649	47.933	-108.567	150	18	2.3	22	24
650	35.267	-106.200	150	18	2.72	51	56
651	44.400	-68.617	150	15	3.89	60	66
652	42.450	-74.450	150	15	2.72	41	45
653	41.384	-105.420	150	15	2.18	33	36
654	41.801	-122.001	150	14	1.21	17	19
655	44.267	-75.400	150	10	4.73	47	51
656	37.867	-118.851	150	9	3.22	30	33
657	44.150	-85.000	150	0	0	50	55
658	44.200	-85.183	150	0	0	46	50
659	44.067	-85.083	150	0	0	54	59
660	34.851	-118.733	150	0	0	61	67
661	36.384	-78.967	149	10	3.77	41	45

Table 5. cont.

662	37.733	-117.180	146	41	2.3	96	105
663	43.451	-115.586	145	46	1.59	73	80
664	40.501	-122.601	145	12	3.05	38	42
665	33.283	-112.618	143	51	2.83	143	156
666	33.283	-112.618	143	50	2.8	143	156
667	33.317	-107.700	143	49	2.13	106	116
668	36.067	-78.117	142	19	3.14	60	66
669	38.050	-107.500	140	89	1.62	44	48
670	38.050	-107.500	140	89	1.59	143	156
671	32.333	-108.851	140	67	1.98	131	143
672	35.217	-107.020	140	56	2.3	130	142
673	36.150	-104.580	140	55	2.09	117	128
674	40.150	-101.480	140	50	1.09	56	61
675	43.968	-116.618	140	45	1.46	66	72
676	42.167	-113.419	140	43	2.38	102	112
677	48.519	-101.200	140	43	1.21	51	56
678	36.033	-107.900	140	41	1.59	66	72
679	32.217	-87.618	140	37	0.96	36	39
680	36.633	-105.650	140	35	3.64	130	142
681	43.018	-116.783	140	33	2.59	87	95
682	32.500	-106.100	140	30	2.38	73	80
683	43.867	-109.280	140	28	2.89	81	89
684	38.950	-108.617	140	27	2.47	67	73
685	48.601	-120.380	140	26	2.85	76	83
686	39.051	-95.467	140	26	1.9	48	52
687	38.317	-117.520	140	25	2.8	70	77
688	35.050	-106.520	140	19	2.26	45	49
689	35.317	-106.170	140	18	3.05	55	60
690	36.867	-77.900	140	18	3.22	58	63
691	40.150	-96.068	140	18	3.18	57	62
692	32.717	-83.250	140	15	2.47	38	42
693	41.168	-105.320	140	15	2.89	46	50
694	36.418	-78.885	139	10	3.47	35	38
695	44.934	-113.470	138	20	3.22	62	68
696	40.033	-118.320	137	91	1.13	104	114
697	47.067	-103.670	137	45	1.2	53	58
698	47.117	-103.670	137	44	1.21	61	67
699	36.767	-115.870	137	33	2.72	92	101
700	39.000	-74.900	137	28	1.55	45	49
701	39.250	-119.670	137	21	3.89	82	90
702	38.917	-119.070	137	20	3.64	75	82
703	40.550	-117.230	137	18	4.77	86	94

Table 5. cont.

704	45.835	-119.670	135	71	1.59	112	122
705	43.884	-122.200	135	65	1.72	115	126
706	45.817	-122.450	135	38	1.59	60	66
707	46.267	-118.750	135	34	1.59	55	60
708	38.233	-79.817	135	17	3.77	66	72
709	45.869	-120.680	134	52	1.42	75	82
710	36.269	-76.201	134	28	1.63	47	51
711	44.053	-122.020	131	89	1.55	139	152
712	36.418	-79.019	131	11	3.64	41	45
713	44.168	-117.380	130	94	1.17	112	122
714	42.317	-117.900	130	70	1.72	121	132
715	42.434	-117.770	130	60	1.59	96	105
716	36.800	-104.950	130	52	1.72	91	100
717	34.100	-106.800	130	42	2.09	90	98
718	46.434	-120.200	130	41	1.59	65	71
719	36.750	-108.800	130	41	1.51	64	70
720	45.518	-122.430	130	37	1.3	48	52
721	37.783	-108.767	130	37	2.59	99	108
722	32.533	-107.680	130	36	4.1	150	164
723	32.333	-108.780	130	33	2.18	74	81
724	35.250	-107.220	130	33	2.26	77	84
725	33.633	-114.333	130	32	3.05	100	109
726	33.467	-105.780	130	30	2.26	69	75
727	33.883	-106.350	130	29	2.18	66	72
728	37.584	-107.585	130	28	3.59	96	105
729	31.753	-109.734	130	27	3.01	81	89
730	41.052	-107.750	130	26	2.51	66	72
731	38.183	-104.733	130	25	4.48	113	124
732	33.102	-111.585	130	25	3.72	93	102
733	36.267	-104.100	130	25	2.51	64	70
734	35.750	-105.650	130	24	3.64	89	97
735	34.734	-117.768	130	23	2.89	64	70
736	43.668	-112.751	130	22	1.38	31	34
737	38.268	-109.300	130	22	0	79	86
738	35.635	-89.818	130	20	2.51	50	55
739	48.352	-118.870	130	20	3.35	68	74
740	39.283	-114.350	130	20	3.77	76	83
741	42.633	-71.417	130	18	3.77	68	74
742	35.300	-106.170	130	16	3.26	52	57
743	41.634	-105.380	130	14	1.67	24	26
744	43.683	-112.300	130	7	1.38	10	11
745	38.367	-98.167	128	40	1.55	63	69

Table 5. cont.

746	33.902	-115.069	128	27	4.06	111	121
747	44.133	-103.720	126	7	2.8	20	22
748	44.350	-112.003	125	67	1.88	125	137
749	46.302	-119.750	125	34	1.59	53	58
750	36.185	-89.651	125	31	2.05	65	71
751	46.536	-122.570	125	25	1.67	38	42
752	37.650	-118.602	125	24	3.31	79	86
753	36.252	-89.485	125	23	2.3	55	60
754	36.302	-78.833	124	11	3.35	40	44
755	41.951	-122.319	122	41	1.8	74	81
756	39.867	-112.050	122	39	2.05	82	90
757	45.834	-122.520	122	38	1.05	40	44
758	34.001	-113.217	122	37	2.13	79	86
759	34.119	-112.851	122	32	2.13	70	77
760	34.067	-114.669	122	30	2.85	85	93
761	34.669	-114.351	122	28	3.35	94	103
762	40.267	-116.750	122	27	3.85	104	114
763	41.200	-78.650	122	26	2.01	54	59
764	40.950	-116.020	122	25	2.8	71	78
765	39.451	-121.985	122	24	1.3	32	35
766	34.550	-117.717	122	24	2.85	69	75
767	33.602	-116.451	122	22	2.47	55	60
768	34.500	-118.269	122	22	2.47	56	61
769	34.883	-118.767	122	22	3.39	76	83
770	40.167	-121.501	122	18	2.43	46	50
771	33.769	-115.919	122	17	3.1	54	59
772	41.852	-123.353	122	16	2.51	41	45
773	35.002	-111.284	122	7	1.59	27	30
774	40.100	-77.183	122	3	6.15	23	25
775	37.351	-75.985	121	25	2.38	61	67
776	37.752	-78.085	121	15	2.59	41	45
777	36.917	-104.870	120	64	2.13	138	151
778	39.717	-113.220	120	55	2.2	121	132
779	35.100	-109.433	120	51	2.13	110	120
780	34.035	-112.350	120	50	1.72	86	94
781	34.035	-111.335	120	50	1.71	85	93
782	35.200	-107.080	120	49	2.34	115	126
783	42.903	-102.200	120	48	1.3	62	68
784	45.701	-120.130	120	45	1.55	54	59
785	32.019	-92.269	120	44	2.38	105	115
786	32.717	-107.580	120	41	2.64	107	117
787	32.283	-106.400	120	41	2.3	95	104

Table 5. cont.

788	42.602	-102.200	120	38	1.67	65	71
789	34.117	-107.280	120	38	2.13	84	92
790	32.719	-91.884	120	37	2.05	76	83
791	36.617	-108.620	120	37	2.47	94	103
792	38.783	-106.167	120	37	2.51	120	131
793	44.003	-111.250	120	36	2.05	75	82
794	32.835	-108.919	120	35	2.5	84	92
795	32.850	-108.300	120	33	2.93	97	106
796	39.002	-95.469	120	32	1.46	48	53
797	45.900	-122.650	120	32	1.3	41	45
798	32.817	-92.735	120	32	2.55	82	90
799	35.300	-106.250	120	31	2.26	71	78
800	38.135	-105.435	120	31	2.13	66	72
801	39.483	-105.734	120	30	3.67	105	115
802	36.517	-104.370	120	30	3.31	102	112
803	40.050	-96.451	120	30	1.67	51	56
804	45.767	-122.190	120	29	2.8	81	89
805	32.967	-107.530	120	29	2.26	68	74
806	46.568	-123.020	120	29	1.59	46	50
807	30.702	-87.001	120	28	1.51	43	47
808	40.952	-100.570	120	28	2.18	63	69
809	40.952	-100.570	120	28	2.18	63	69
810	44.003	-112.485	120	28	1.46	42	46
811	31.452	-91.334	120	27	2.09	58	63
812	34.734	-118.385	120	27	2.59	71	78
813	47.767	-117.170	120	27	3.26	88	96
814	43.784	-115.835	120	26	3.01	79	86
815	46.601	-120.380	120	26	1.59	41	45
816	38.267	-105.517	120	26	2.68	70	77
817	45.700	-121.230	120	26	1.59	41	45
818	33.000	-92.736	120	24	2.51	63	69
819	44.067	-71.167	120	24	3.26	79	86
820	30.434	-91.135	120	23	2.13	51	56
821	40.551	-111.670	120	23	3.26	72	79
822	32.352	-89.500	120	21	1.55	33	36
823	43.633	-71.517	120	21	2.68	58	63
824	47.669	-121.640	120	20	3.01	60	66
825	43.483	-72.083	120	19	2.76	53	58
826	48.352	-118.870	120	19	3.35	65	71
827	46.334	-112.070	120	19	3.93	76	83
828	46.351	-122.070	120	18	3.68	68	74
829	48.051	-118.700	120	17	4.14	74	81

Table 5. cont.

830	32.801	-90.918	120	17	1.92	33	36
831	31.067	-104.780	120	16	4.85	76	83
832	43.334	-112.936	120	10	1.38	15	16
833	43.786	-112.185	120	8	1.34	10	11
834	34.751	-83.135	119	16	3.47	56	61
835	34.350	-114.167	118	28	2.13	61	67
836	37.351	-75.985	118	24	2.22	55	60
837	43.235	-112.000	117	38	1.88	71	78
838	42.317	-118.620	116	173	1.09	187	205
839	42.667	-115.853	115	101	1.51	152	166
840	46.086	-121.700	115	53	1.21	66	72
841	38.468	-94.901	115	52	1.13	59	65
842	40.200	-101.150	115	48	1.09	53	58
843	38.967	-104.883	115	36	2.18	80	88
844	34.650	-117.836	115	25	1.09	65	71
845	41.485	-96.551	115	23	2.38	55	60
846	48.051	-118.700	115	19	3.81	74	81
847	47.001	-121.690	115	19	2.38	46	50
848	34.218	-116.401	115	16	2.85	46	50
849	41.883	-71.133	115	13	3.85	51	56
850	41.883	-71.133	115	13	3.85	51	56
851	38.917	-121.601	114	20	1.42	28	31
852	37.335	-80.767	113	18	6.07	114	125
853	36.403	-77.902	111	18	2.72	50	55
854	45.368	-109.900	111	16	3.51	56	61
855	35.933	-106.670	110	239	1.76	42	46
856	44.151	-117.400	110	99	1.17	117	128
857	34.251	-116.135	110	80	1.26	99	108
858	32.219	-112.719	110	47	1.84	87	95
859	36.450	-105.580	110	41	2.34	98	107
860	46.352	-119.270	110	40	1.59	63	69
861	36.817	-104.680	110	38	2.3	89	97
862	46.336	-117.002	110	38	1.72	66	72
863	33.950	-106.930	110	34	2.09	72	79
864	38.767	-106.469	110	32	2.93	85	93
865	43.902	-111.467	110	32	1.55	49	54
866	43.902	-111.467	110	32	1.55	49	54
867	38.233	-117.550	110	31	3.05	96	105
868	37.634	-118.683	110	30	3.1	93	102
869	33.051	-111.384	110	28	2.93	82	90
870	46.534	-122.820	110	27	1.09	29	32
871	33.534	-116.601	110	26	2.8	73	80

Table 5. cont.

872	46.383	-112.570	110	26	3.1	80	88
873	30.534	-104.430	110	25	1.88	49	54
874	35.517	-106.120	110	23	2.13	51	56
875	33.518	-116.801	110	22	2.76	61	67
876	43.450	-71.733	110	20	1.92	38	42
877	40.851	-95.802	110	20	2.18	44	48
878	40.851	-95.802	110	20	2.18	44	48
879	46.633	-123.220	110	20	1.97	41	45
880	41.417	-106.250	110	19	2.64	50	55
881	43.083	-72.367	110	14	4.14	59	65
882	47.418	-121.400	110	14	2.97	43	47
883	42.736	-113.401	110	12	1.38	17	19
884	38.785	-110.680	110	10	4.73	51	56
885	47.752	-118.520	109	55	1.59	87	95
886	46.568	-114.030	109	40	2.34	96	105
887	33.533	-112.333	107	50	3.47	125	137
888	47.467	-103.800	107	42	1.21	51	56
889	32.435	-106.090	107	40	2.3	93	102
890	37.717	-117.780	107	34	2.26	77	84
891	33.417	-112.017	107	29	1.55	46	50
892	38.933	-119.070	107	22	3.35	77	84
893	38.933	-119.070	107	22	3.43	77	84
894	37.750	-77.550	107	18	3.18	58	63
895	33.435	-115.134	107	15	2.38	36	39
896	43.018	-114.719	105	94	1.55	146	160
897	44.168	-117.420	105	70	1.17	83	91
898	42.319	-120.520	105	70	0.88	66	72
899	45.602	-122.120	105	63	1.05	66	72
900	44.101	-122.220	105	52	1.59	83	91
901	42.434	-98.650	105	50	1.17	59	65
902	33.250	-96.650	105	44	1.13	51	56
903	38.233	-104.933	105	38	2.13	83	91
904	45.602	-122.180	105	36	1.05	37	40
905	42.401	-120.480	105	32	0	58	63
906	44.183	-112.436	105	29	2.43	71	78
907	44.035	-111.684	105	21	1.46	31	34
908	42.803	-122.930	105	20	2.93	61	67
909	43.017	-71.617	105	20	3.35	68	74
910	43.818	-112.735	105	11	1.46	17	19
911	42.302	-118.650	104	56	1.17	66	72
912	48.419	-119.500	104	27	1.97	53	58
913	33.468	-83.033	104	19	3.31	64	70

Table 5. cont.

914	35.784	-78.417	104	16	3.05	51	56
915	44.169	-112.517	102	59	2.43	143	157
916	41.569	-122.869	102	16	2.38	38	42
917	45.451	-121.640	101	31	1.76	56	61
918	45.451	-121.640	101	21	1.76	38	42
919	43.050	-115.317	100	98	1.38	136	149
920	44.200	-122.040	100	88	1.72	153	167
921	36.767	-105.970	100	74	2.01	150	164
922	43.217	-118.730	100	68	0.96	66	72
923	45.384	-121.800	100	64	2.09	133	146
924	35.117	-109.350	100	58	2.76	158	173
925	43.652	-112.867	100	58	1.34	43	47
926	45.384	-121.850	100	57	1.51	87	95
927	42.786	-115.251	100	55	1.88	104	114
928	44.317	-111.451	100	52	1.63	87	95
929	45.968	-121.620	100	52	1.42	74	81
930	47.751	-118.700	100	52	1.59	84	92
931	42.500	-118.120	100	51	1.17	60	66
932	45.634	-121.970	100	49	1.38	69	76
933	45.986	-121.890	100	49	1.21	61	67
934	35.667	-106.180	100	48	2.22	108	118
935	32.167	-109.030	100	47	2.55	122	134
936	37.767	-103.617	100	46	1.97	92	101
937	32.783	-109.383	100	45	2.01	87	95
938	45.301	-121.670	100	45	2.51	114	125
939	33.317	-111.717	100	44	1.55	71	78
940	41.452	-103.750	100	43	1.09	47	51
941	46.518	-120.320	100	41	1.59	66	72
942	33.567	-107.600	100	41	1.97	82	90
943	38.135	-105.435	100	40	1.72	69	76
944	32.285	-90.185	100	39	1.38	53	58
945	37.433	-106.600	100	39	2.64	102	112
946	32.285	-90.183	100	38	1.38	53	58
947	41.883	-115.080	100	37	3.64	138	151
948	39.950	-108.383	100	37	1.59	59	65
949	38.217	-105.017	100	36	2.34	85	93
950	36.033	-107.900	100	36	1.72	63	69
951	32.285	-90.183	100	35	1.38	48	53
952	46.084	-118.330	100	35	1.59	56	61
953	45.651	-121.320	100	35	1.59	55	60
954	32.417	-106.120	100	34	2.64	92	101
955	43.201	-105.070	100	34	2.03	69	76

Table 5. cont.

956	46.534	-122.820	100	34	1.09	37	41
957	41.850	-109.530	100	34	2.05	71	78
958	38.135	-105.435	100	34	1.88	66	72
959	32.819	-92.135	100	34	2.68	94	103
960	39.650	-105.734	100	34	3.55	109	119
961	46.534	-122.830	100	33	1.09	35	38
962	41.850	-109.530	100	33	2.05	67	73
963	44.134	-112.935	100	33	1.46	49	54
964	47.817	-118.020	100	33	2.51	84	92
965	46.519	-122.800	100	32	1.09	35	38
966	32.035	-88.267	100	32	1.09	35	38
967	33.084	-111.400	100	31	2.89	92	101
968	41.386	-79.718	100	31	2.64	83	91
969	37.533	-104.900	100	31	2.55	81	89
970	45.686	-123.120	100	31	1.3	41	45
971	31.883	-111.133	100	30	2.76	83	91
972	45.435	-121.700	100	30	1.55	46	50
973	39.767	-105.833	100	29	3.35	82	90
974	39.767	-105.833	100	29	3.38	83	91
975	39.467	-105.783	100	29	3.35	97	106
976	38.135	-105.435	100	29	2.26	68	74
977	39.867	-105.550	100	28	2.43	69	76
978	35.333	-107.620	100	28	2.26	64	70
979	33.401	-90.819	100	28	1.88	55	60
980	34.502	-88.967	100	28	1.17	33	36
981	46.934	-110.485	100	28	2.43	69	76
982	42.153	-121.670	100	28	0.75	20	22
983	38.985	-107.051	100	27	3.1	87	95
984	36.650	-107.670	100	27	1.92	52	57
985	35.368	-89.550	100	27	2.76	74	81
986	45.435	-121.700	100	27	1.55	41	45
987	31.885	-92.667	100	27	2.38	66	72
988	32.600	-111.600	100	26	1.38	35	38
989	32.850	-90.402	100	26	2.68	71	78
990	36.600	-107.420	100	25	1.97	50	55
991	44.434	-111.484	100	25	1.63	41	45
992	45.268	-121.830	100	25	2.64	66	72
993	47.935	-118.150	100	25	2.97	75	82
994	33.400	-91.083	100	25	1.97	50	55
995	34.201	-90.535	100	24	2.97	73	80
996	33.935	-90.767	100	23	2.01	48	53
997	32.800	-108.070	100	23	2.76	66	72

Table 5. cont.

998	47.034	-112.368	100	23	3.68	87	95
999	36.367	-106.900	100	23	2.72	65	71
1000	43.417	-84.617	100	22	2.09	46	50
1001	41.685	-94.168	100	22	2.18	48	53
1002	30.417	-91.134	100	22	2.05	46	50
1003	42.368	-107.820	100	22	2.89	66	72
1004	35.567	-105.250	100	22	2.68	60	66
1005	42.783	-72.133	100	21	3.18	68	74
1006	44.734	-116.783	100	21	2.8	61	67
1007	45.934	-122.700	100	21	1.72	37	41
1008	35.250	-107.220	100	21	3.51	74	81
1009	39.783	-105.267	100	20	2.97	63	69
1010	35.103	-89.933	100	20	2.72	56	61
1011	48.917	-117.580	100	20	5.98	124	136
1012	34.784	-88.417	100	20	2.51	53	58
1013	32.267	-90.067	100	19	2.38	46	50
1014	34.618	-89.967	100	19	2.09	41	45
1015	44.386	-114.317	100	19	4.27	81	89
1016	46.769	-122.250	100	19	1.72	33	36
1017	35.151	-90.017	100	18	2.76	51	56
1018	38.983	-120.317	100	18	2.85	52	57
1019	41.384	-91.903	100	18	3.47	62	68
1020	44.333	-74.267	100	18	1.84	33	36
1021	41.201	-91.318	100	18	3.22	61	67
1022	38.236	-109.280	100	18	0	64	70
1023	33.802	-116.168	100	18	2.72	49	54
1024	40.901	-86.452	100	17	3.26	58	63
1025	41.352	-91.901	100	17	3.47	62	68
1026	43.751	-112.217	100	17	1.34	23	25
1027	33.100	-91.034	100	17	1.88	33	36
1028	40.751	-87.784	100	16	3.68	60	66
1029	29.633	-81.633	100	16	2.18	33	36
1030	42.501	-107.650	100	16	3.68	61	67
1031	45.303	-121.790	100	16	2.22	36	39
1032	40.917	-86.450	100	15	3.72	58	63
1033	28.067	-82.783	100	15	1.84	29	32
1034	41.700	-71.167	100	15	4.14	61	67
1035	32.334	-88.601	100	15	2.22	35	38
1036	40.884	-86.468	100	14	4.1	58	63
1037	40.752	-87.801	100	14	4.1	58	63
1038	41.652	-94.152	100	14	3.43	48	53
1039	41.700	-71.167	100	14	4.14	60	66

Table 5. cont.

1040	33.169	-88.468	100	14	3.01	43	47
1041	41.383	-86.233	100	14	3.81	53	58
1042	37.335	-118.551	100	14	3.68	53	58
1043	41.552	-94.101	100	13	3.64	48	53
1044	33.685	-89.703	100	13	2.68	35	38
1045	42.418	-83.552	100	12	4.52	58	63
1046	41.017	-88.885	100	12	4.81	58	63
1047	33.418	-88.386	100	12	1.51	19	21
1048	35.183	-89.851	100	12	2.55	33	36
1049	33.617	-88.635	100	12	1.09	13	14
1050	35.018	-90.118	100	12	2.47	30	33
1051	40.802	-87.885	100	11	5.1	59	65
1052	42.718	-85.817	100	11	3.77	44	48
1053	42.619	-94.036	100	11	3.39	40	44
1054	44.050	-85.084	100	11	3.97	46	50
1055	34.769	-88.567	100	11	1.72	20	22
1056	42.618	-94.051	100	10	3.51	38	42
1057	42.633	-94.017	100	10	3.51	38	42
1058	42.633	-94.018	100	10	3.51	37	41
1059	36.083	-83.650	100	10	3.26	34	37
1060	35.001	-84.384	100	10	2.72	28	31
1061	35.235	-89.951	100	10	2.47	26	28
1062	44.000	-72.083	100	9	4.14	41	45
1063	40.968	-84.867	100	8	4.64	40	44
1064	33.933	-85.833	100	7	1.3	10	11
1065	37.819	-118.802	100	6	2.8	17	19
1066	42.733	-86.000	100	0	0	37	41
1067	42.733	-86.000	100	0	0	37	41
1068	42.733	-86.000	100	0	0	37	41
1069	43.800	-82.733	100	0	0	33	36
1070	43.533	-85.267	100	0	0	50	55
1071	43.533	-85.600	100	0	0	41	45
1072	43.701	-112.917	100	0	1.34	11	12

REFERENCES

Beck, A. E. 1965. Techniques for measuring heat flow on land. In W. H. K. Lee, (Ed.). *Terrestrial heat flow*. American Geophysical Union Geophysical Monograph 8, p. 24-57.

Beck, A. E. 1977. Climatically Perturbed Temperature Gradients and their effects on regional and continental heat flow means. *Tectonophysics, 41*, 17-39.

Beltrami, H., & Mareschal, J. C. 1991. Recent temperature changes in eastern Canada inferred from geothermal measurements. *Geophys. Res. Lett., 18*, 605-608.

Benfield, A. F. 1939. Terrestrial heat flow in Great Britain. *Proc. R. Soc. London, Ser. A, 173*, 428-450.

Birch, F. 1948. The effects of Pleistocene climatic variations upon geothermal gradients. *Am. J. Sci., 246*, 729-760.

Birch, F. 1950. Flow of heat in the front range, Colorado. *Geological Society of American Bulletin, 61*(6), 567-630.

Blackwell, D. D. 1971. The Thermal Structure of the Continental Crust. In J. G. Heacock, (Eds.). *The Structure and Physical Properties of the Earth's Crust: American Geophysical Union Monograph, 14*, 169-184.

Blackwell, D. D. 1978. Heat Flow and Energy Loss in Western United States, p. 175-208, in R. B. Smith G. P. Eaton, (Eds.). *Cenozoic Tectonics and Regional Geophysics of the Western Cordillera*, ed. *Geol. Soc. Amer. Mem.* 152, 388 pp.

Blackwell, D. D., Steele, J. L., & Carter, L. S. 1991. Heat Flow Patterns of the North American Continent; A discussion of the Geothermal Map of North America. In D. B. Slemmons, E. R. Engdahl, M. D. Zoback, & D. D. Blackwell (Eds.). *Neotectonics of North America*, (pp. 423-437). Geological Society of America, Boulder, Colorado, Decade Map vol. 1, 498 pp.

Blackwell D. D., & Richards, M. 2004. Geothermal Map of North America, American Association of Petroleum Geologists, Tulsa, Oklahoma.

Bullard, E. C. 1939. Heat Flow in South Africa, Proc. Roy. Soc. London, Ser. A, 173, 474-502.

Carslaw & Jaeger. 1959. *Conduction of Heat in Solids* (p. 510). New York: Oxford University Press.

Cermak, V. 1971. Underground temperature and inferred climatic temperature of the past millennium. *Palaeogeogr., Palaeoclimatol., Palaeoecol. 10*, 1-19.

Cermak, V., Bodri, L., & Safanda, J. 1992. Underground temperature fields and changing climate: Evidence from Cuba. *Global and Planetary Change, 97*, 325-327.

Clauser, C., & Mareschal, J. C. 1995. Ground temperature history in Central Europe from borehole temperature data. *Geophys. J. Int. 121*(3): 805-817.

Clow, G. D. 1998. Reconstructing Past Climatic Changes in Greenland and Antarctica from Borehole Temperature Measurements [Abstract]. *EOS Trans. Am. Geophys. Union 79*, F833.

Cranganu, C., Youngmin, L., & Deming, D. 1998. Heat flow in Oklahoma and the south central United States. *J. Geophys. Res., 103*(27), 107–27,121.

Deming, D. 1995. Climatic warming in North America: Analysis of borehole temperatures. *Science, 268*, 1576-1577.

ESRI (Environmental Systems Resource Institute). 2013. ArcMap 10. ESRI, Redlands, California.

Ganopolski, A., Rahmstorf, S., Petoukhov, V., & Claussen, M. 1998. Simulation of modern and glacial climates with a coupled global model of intermediate complexity: *Nature, 391*, 351-356.

Gosnold, W. D. 1990. Heat flow in the Great Plains of the United States. *Journal of Geophysical Research, 95*(1), 353-374.

Gosnold, W. D., & LeFever, R. D. 1991. Comparison of climate records with borehole temperatures in the Central United States. *EOS, 72*, 69.

Gosnold, W. D., Todhunter, P. E., & Schmidt, W. 1997. The borehole temperature record of climate warming in the mid-continent of North America. *Global and Planetary Change, 15*(1-2), 33-45

Gosnold, W. D, Majorowicz, J., Šafanda, J., & Szewczyk, J. 2005. Has northern hemisphere heat flow been underestimated? American Geophysical Union, Spring Meeting 2005, May 23–27, New Orleans, LA, abstract #T43D-01.

Harris, R. N., & Chapman, D. S. 1995. Climate change on the colorado plateau of eastern Utah Inferred from borehole temperatures. *J. Geophys. Res., 100*, 6367-6381.

Holland, M. M., & Bitz, C. M. 2003. Polar Amplification of Climate Change in Coupled Models. *Climate Dynamics, 21*, 221-232.

Hotchkiss, W. O, & Ingersoll, L. R. 1934. Post-glacial time calculations from recent geothermal measurements in the Calumet copper mines. *Journal of Geology, 42,* 113-142.

Huang, S., Pollack, H. N., & Shen, P. Y. 1997. Late quaternary temperature changes seen in world wide continental heat flow measurements. *Geophys. Res. Lett. 24,* 1947-1950.

Jessop, A. 1971. The distribution of glacial perturbation of heat flow in Canada. *Canadian Journal of Earth Sciences, 8*, 162–166.

Kappelmeyer, O., & Haenel, R, 1974. Geothermics with Special reference to application. Berlin, GebrÜder Borntraeger, 238 p.

Kukkonen, I., Gosnold, W. D., & Safanda, J. 1998. Anomalously low heat flow density in eastern Karelia, Baltic Shield; a possible palaeoclimatic signature, *Tectonophysics, 291*(1-4), 235-249.

Kukkonen, I., & Joeleht, A. 2003. Weichselian temperatures from geothermal heat flow data. J. *Geophys. Res. 108*(B3): 2163, 325,doi:10.1029/2001JB001579

Lachenbruch, A. H. 1970. Crustal Temperature and heat production: Implications of the Linear heat-flow relation. *Journal of Geophysical Research, 75*(17), 3291-3300.

Lachenbruch, A. H., & Sass, J. H. 1978. Heat flow in the United States and thermal regime of the crust. In J. G. Heacock, (Ed.). *The Nature and Physical Properties of the Earth's Crust*, American Geophysical Union Monograph. 20, p. 626-675.

Lachenbruch, A. H., & Sass, J. H. 1980. Heat flow and energetics of the San Andreas Fault Zone. *Journal of Geophysical Research, 90,* 6185-6222.

Lachenbruch, A. H., & Marshall, B. V. 1986. Changing climate: Geothermal Evidence from permafrost in the Alaskan Arctic, *Science, 234,* 689-696.

Lachenbruch, A. H., & Sass, J. H. 1992. Heat flow from Cajon Pass, fault strength and tectonic implications. *Journal of Geophysical Research, 97,* 4995-5016.

Langseth, M. G. 1965. Techniques of Measuring Heat Flow through the Ocean Floor. In W. H. K. Lee (Ed.). *Terrestrial Heat Flow, American Geophysical Union Geophysical Monograph 8,* 58-77.

Majorowicz, J. A, & Safanda, J. 1998. Ground surface temperature history from inversions of underground temperatures - A case study of the Western Canadian sedimentary basin. *Tectonophysics, 291,* 287-298.

Majorowicz, J., & Wybraniec, S. 2011. New terrestrial heat flow map of Europe after regional paleoclimatic correction application. *International Journal of Earth Science 100,* 881-887.

Morgan, P., & Gosnold, W. D. 1989. Heat Flow and Thermal Regimes in the Continental United States, p. 493-523. In L. C. Pakiser, and W. D. Mooney (Eds.). *Geophysical Framework of the Continental United States*, Geological Survey American Memoir 172, 826 pp.

National Climatic Data Center. 2013. National Oceanic and Atmospheric Administration. 13 July 2013 <http://www.ncdc.noaa.gov/cag/.

Ochoa, G., Hoffman, J., & Tin, T. 2005. Climate: The force that shapes our world and the future of life on earth. Emmaus, PA: Rodale. ISBN 1-59486-288-5. p 92.

Pollack, H. N., & Chapman, D. S. 1993. Underground records of changing climate. *Sci. Am. 268,* 44-50.

Reiter, M., Barroll, & Minier, J. 1991. An overview of Heat Flow in Southwestern Unites States and Chihuahua, Mexico, p. 457-466. In D. B. Slemmons, E. R. Engdahl, M. D. Zoback, & D. D. Blackwell (Eds.). *Neotectonics of North America*. Geological Society of America, Decade of North American Geology, Decade Map vol. 1, 498 pp.

Ritchie, J. C. 1983. The paleoecology of the central and northern parts of the glacial Lake Agassiz basin. *Geological Association of Canada, Special Paper, 26*, 157-170.

Rolandone, F., Mareschal, J.-C., Jaupart, C., Gosselin, C., Bienfait, G., & Lapointe, R. 2003. Heat flow in the western superior province of the Canadian Shield. *Geophysical Research Letters, 30,* 4.

Roy, R. F., Blackwell, D. D., & Decker, E. R. 1972. Continental Heat Flow. In E. C. Robertson (Ed.). *The Nature of the Solid Earth*, New York, McGraw-Hill, p. 506-543.

Safanda, J., Szewczyk, J., & Majorowicz, J. 2004. Geothermal evidence of very low glacial temperatures on a rim of the Fennoscandian Ice Sheet. *Geophysical Research Letters*, Vol. 31.L07211, doi:10.1029/2004GL019547.2004

Sass, J. H., Lachenbruch, A. H., & Monroe, R. J. 1971. Thermal conductivity of rocks from measurement on fragments and its application to heat flow determinations. *Journal of Geophysical Research, 76*, 3391-3401.

Sass, J. H., Lachenbruch, A. H., Munroe, R. J., Greene, G. W., & Moses, Jr. T. H. 1971. Heat flow in the western United States. *Journal of Geopysical Research, 76*, 6376-6413.

Sclater, J. G., Jaupart, C., & Galson, D. 1980. The Heat flow through oceanic and continental crust and the heat loss of the Earth. *Reviews of Geophysics and Space Physics, 18*(1), 269-311.

Shen, P. Y., Pollack, H. N., & Huang, S. 1996. Inference of Ground Surface Temperature History from Borehole Temperature Data: A comparison of two inverse method, *Global and Planetary Change, 14*(1-2), 49-57.

SMU-UND United States Heat Flow Database 2013

Slagstad, T., Balling, N., Elvebakk, H., Midttomme, K., Olesen, O., Olesen, L., & Pascal, C. 2009. Heat flow measurements in Late Palaeoproterozoic to Permian Geological Provinces in South and Central Norway and a new heat flow map of Fennoscandia and Norwegian-Greenland Sea. *Tectonophysics 473*, 341-361.

Wang, K. 1992. Estimation of ground surface temperatures from borehole temperature data. *J. Geophys. Res., 97*, 2095-2106.

Wang, K., & Lewis, T. J. 1992. Geothermal evidence from Canada for a cold period before recent climate warming, *Science, 256*, 1003-1005.

Westaway, R., & Younger, P. L. 2013. Accounting for palaeoclimate and topography: A rigorous approach to correction of the British geothermal dataset. *Geothermics 48*, 31-51.

Wisian, K. W., Blackwell, D. D, & Richards, M. 1999. Heat flow in the western United States and extensional geothermal systems, Proceedings of the 24th Workshop on Geothermal Reservoir Engineering, Stanford University.